Decreased concentrations of retinol-binding protein 4 in sera of epithelial ovarian cancer patients: A potential biomarker identified by proteomics

LUCIE LORKOVA[1], JANA POSPISILOVA[1], JAN LACHETA[2], SERGIU LEAHOMSCHI[1], JAROSLAV ZIVNY[2], DAVID CIBULA[2], JAN ZIVNY[1] and JIRI PETRAK[1,3]

[1]Institute of Pathological Physiology, and [2]Department of Gynecology and Obstetrics, First Faculty of Medicine, Charles University, Prague; [3]Institute of Hematology and Blood Transfusion, Prague, Czech Republic

Received August 29, 2011; Accepted September 30, 2011

DOI: 10.3892/or.2011.1513

Abstract. Ovarian cancer is the fifth leading cause of cancer death in women. Absence of a reliable biomarker precludes early diagnosis of the disease. To identify new proteins with potential diagnostic or prognostic value for the therapy of ovarian cancer we performed comparative proteomic analysis of sera from ovarian cancer patients and healthy women. We analyzed serum samples from 10 patients diagnosed with epithelial ovarian cancer and 10 age-matched healthy women. To decrease the extremely wide dynamic range of protein concentrations in serum we used combinatorial hexapeptide libraries. Serum samples were then subjected to proteomic 2-DE analysis. Three proteins with differential abundance were found and identified by mass spectrometry: α-1-antitrypsin, apolipoprotein A-IV and retinol-binding protein 4. Identification of α-1-antitrypsin and apolipoprotein A-IV confirms previous studies but the identification of significantly decreased levels of RBP4 in ovarian cancer patients represents a novel observation. We verified the decrease of RBP4 levels in ovarian cancer patient sera by two independent methods and determined absolute RBP4 concentrations in patients and healthy women. We excluded possible non-cancer factors that could be responsible for the observed RBP4 decrease. We propose a connection of RBP4 with epithelial ovarian cancer and advocate the potential of RBP4 as a candidate diagnostic or prognostic biomarker.

Correspondence to: Dr Jiri Petrak, Institute of Pathological Physiology, First Faculty of Medicine, Charles University in Prague, U Nemocnice 5, 120 00 Prague, Czech Republic
E-mail: jpetr@lf1.cuni.cz

Abbreviations: EOC, epithelial ovarian cancer; FIGO, International Federation of Gynecology and Obstetrics; IUCC, International Union against Cancer; ELISA, enzyme-linked immunosorbent assay; BMI, body-mass index; RBP4, retinol-binding protein 4; TTR, transthyretin; PBS-T, phosphate-buffered saline with 0.1% Tween-20

Key words: ovarian carcinoma, proteomics, combinatorial hexapeptide libraries, biomarkers, retinol-binding protein, cachexia

Introduction

Epithelial ovarian cancer (EOC) is the fifth leading cause of cancer death in women. While overall 5-year survival is only 16-40%, in patients with early stage (FIGO I) ovarian cancer survival rate is 95% (1,2). Unfortunately, vast majority of the patients is diagnosed in advanced stage disease (FIGO III/IV), mostly because of absence of specific symptoms and by lack of reliable serum markers for early disease. Effective screening tests are yet to be developed.

The most widely used serum marker for ovarian cancer, mucin protein CA125, has low sensitivity, its serum concentration is increased in less than half of early stage patients. Furthermore, its specificity is also insufficient, increased levels have been reported also in patients with benign gynecological diseases, endometriosis, cirrhosis and heart disease (3). Enormous effort has therefore been developed to identify and implement new serum biomarkers with sufficient sensitivity and specificity for detection and monitoring of epithelial ovarian cancer. Several candidate molecules have been discovered (4,5). Unfortunately, none of the identified proteins or peptides proved to be of sufficient sensitivity and specificity as a clinically applicable diagnostic marker.

Comparative proteomic analyses of serum or plasma are, among other obstacles, hindered by extremely high dynamic range of individual protein concentration in serum exceeding 10 orders of magnitude (6). Effective methods to decrease the concentration range of serum proteins are based on either immunodepletion of the most abundant serum/plasma proteins or, more recently, on equalization of protein concentrations by interaction with combinatorial hexapeptide library coupled to beads (7,8). The latter method has gained attention under commercial name ProteoMiner™ and was used in our current study. Equalized samples were then subjected to 2-DE differential proteomic analysis. We identified three proteins that were present in serum of EOC patients in concentrations significantly different than in sera of age-matched healthy women. Two of the proteins have been identified in EOC patients previously. Identification of retinol binding protein 4 (decreased in sera of EOC patients) is a novel observation; therefore its altered concentrations were further tested, verified and quantified in individual serum samples.

Materials and methods

All chemicals were from Sigma-Aldrich, unless stated otherwise. The study was approved by the Ethics Committee of the Charles University in Prague, First Faculty of Medicine (IRB approval IGA MZ CR 1.LF UK 19/05).

EOC patient selection. Serum samples were collected at the Department of Gynecology and Obstetrics of the First Faculty of Medicine and General Teaching Hospital after informed consent from both patients and healthy age-matched women after overnight fasting. Patient samples were collected at the time of preliminary diagnosis before surgery and chemotherapy. The diagnosis was confirmed histologically after the surgery and only the samples from patients with confirmed EOC were included in the study. Tumor typing and staging were performed by the Department of Pathology according to the criteria of the International Federation of Gynecologists and Obstetricians (FIGO) and the International Union against Cancer (IUCC).

Serum and plasma collection. Blood was collected into BD Vacutainer tubes (BD, USA) with sodium heparin (plasma) and without additives (serum). The tubes were kept at room temperature for 5 min and centrifuged at 1500 x g for 5 min. Collected plasma was then re-centrifuged at 15000 x g for 20 min to remove remaining platelets. The serum and plasma were aliquoted into 2 ml screw cap tubes (Axygen, USA) and stored at -80˚C.

Serum equalization - hexapeptide ligand library treatment. Concentration of the most abundant serum proteins was reduced using the ProteoMiner Enrichment Kit (Bio-Rad Laboratories, CA, USA). Pooled sera from control healthy women (controls, n=10) and EOC patients (patients, n=10) were used as a starting material (10 ml each pool). To obtain sufficient amount of equalized sera, 10 depletions were performed from each pooled sample, each depletion with a fresh ProteoMiner column and 1 ml of pooled sera. The procedure was carried out according to the manufacturer's instructions. Serum samples relatively enriched in medium- and low-abundant proteins were eluted and pooled. The combined equalized samples (2.7 ml), were precipitated by 40 ml of cold acetone at -20˚C overnight.

Two-dimensional electrophoresis. Precipitated equalized serum protein pellets were dissolved each in 2.8 ml of rehydration buffer (7 M urea, 2 M thiourea, 4% CHAPS, 60 mM DTT, 1% ampholytes (GE, USA) and 0.002% bromophenol blue). Protein concentration was determined and adjusted to 4.4 mg/ml. IPG strips (24 cm, pH 4-7, GE, USA) were rehydrated overnight in 450 μl of the sample, representing 2 mg protein per strip. Six technical replicates were run for each sample.

Isoelectric focusing was performed with a Bio-Rad Protean IEF cell for 80 kVh, with maximum voltage not exceeding 5 kV, current limited to 50 μA per strip and temperature set to 20˚C. Strips were equilibrated and reduced in equilibration buffer A (6 M urea, 50 mM Tris pH 8.8, 30% glycerol, 2% SDS and 450 mg DTT per 50 ml of the buffer) for 15 min and then alkylated in equilibration buffer B (6 M urea, 50 mM Tris pH 8.8, 30% glycerol, 2% SDS and 1.125 mg iodacetamide per 50 ml). Equilibrated strips were then placed on the top of 11% SDS-PAGE and secured in place by molten agarose. Electrophoresis was performed in a Tris-glycine-SDS system using a 12 gel Protean Plus Dodeca Cell apparatus (Bio-Rad) with buffer circulation and external cooling (20˚C). Gels were run at constant voltage of 200 V for 6 h. Following electrophoresis gels were washed 3 times for 15 min in deionized water to remove SDS. Washed gels were stained in CBB (Simply Blue SafeStain, Invitrogen, Carlsbad, USA) overnight and then destained in deionized water.

Gel image analysis. Stained gels were scanned with a GS 800 calibrated densitometer (Bio-Rad). Image analysis was performed with Progenesis PG200/PG220 (Nonlinear Dynamics, UK) in semi-manual mode with six gel replicates for each group. Normalization of gel images was based on total spot density, and integrated spot density values (spot volumes) were calculated after background subtraction. Average spot volume values (averages from the all 6 gels in the group) for each spot were compared between the groups. Protein spots were considered differentially expressed if they met both of the following criteria: average normalized spot volume difference >2-fold and statistical significance ($p<0.05$) of the change determined by the t-test.

MALDI mass spectrometry, protein identification. Differentially expressed proteins were excised from gels, cut into small pieces and washed four times with 25 mM ammonium bicarbonate in 50% acetonitrile. The supernatant was removed and the gel was partially dried in a SpeedVac concentrator. Gel pieces were then reconstituted in a cleavage buffer containing 25 mM ammonium bicarbonate and sequencing grade trypsin (5 ng/ml; Promega, WI, USA). After overnight digestion, the resulting peptides were extracted with 50% ACN/0.1% TFA. Extracted peptide mixture (0.5 μl) was deposited on a steel MALDI target an allowed to air-dry at room temperature. After complete evaporation, 0.5 μl of the matrix solution [α-cyano-4-hydroxycinnamic acid in aqueous 50% ACN/0.1% TFA (5 mg/ml)] was added. MALDI mass spectra were measured on Autoflex II instrument (Bruker Daltonics, Bremen, Germany).

Spectra were acquired in the mass range between ~700 and 3200 Da and calibrated internally using the monoisotopic $[M+H]^+$ ions of Peptide calibration standard II (Bruker Daltonics, Bremen, Germany). Peak lists in XML data format were created using the flexAnalysis 3.1 program with the SNAP peak detection algorithm. No smoothing was applied, and the maximal number of assigned peaks was set to 50. After peak labeling, all known contaminant signals were manually removed. The peak lists were searched using the MASCOT search engine against the SwissProt 2009_11 database subset of human proteins with the following search settings: peptide tolerance 50 ppm, 1 missed cleavage, fixed carbamidomethylation of cystein, variable acetylation of protein N-term and oxidation of methionine. No restrictions on protein molecular weight or pI value were applied. Proteins with a Mascot score over the threshold 55 for $p<0.05$ calculated for the used settings were considered as identified.

Western blotting. Individual serum samples (10 μg of proteins) were combined with SDS loading buffer containing DTT, boiled 5 min and separated on 10% SDS-PAGE minigels in Tris-glycine-SDS buffer. Electrophoresis was performed using

Table I. Details on patients included in the proteomic analysis study.

Patients	Age	BMI[a]	Tumor size	Node involvement	Metastases status	Grade	Histology	Stage	CA125 (U/ml)	RBP4 (μg/ml)
P1	44	17.2	pT3b	pNx	M0	G3	Serous	III	917	32.3
P2	46	29.7	pT3c	pNx	M0	G3	Serous	III	4100	8.1
P3	49	24.4	pT3b	N0	M0	G2	Serous	III	149	27.8
P4	54	21.5	pT1c	pNx	M0	G1	Mucinous	I	350	32.1
P5	59	25.7	pT1c	pN0	M0	G3	Serous	I	19	45.4
P6	55	21.3	pT1c	pN1	M0	G3	Clear cell	III	318	31.5
P7	56	24.0	pT3c	pN1	M0	G3	Serous	III	1685	35.7
P8	56	27.7	pT3c	pNx	M0	G3	Mixed	III	2500	27.2
P9	58	19.9	pT3c	pN1	M0	G1	Serous	III	592	35.9
P10	59	25.4	pT3c	pN1	M1	G2-3	Serous	IV	364	23.2
Mean ± SD	53.6±5.3	23.7±3.8								

[a]BMI, body mass index.

Table II. Details on healthy controls included in the proteomic analysis study.

Healthy controls	Age	BMI[a]	RBP4 (μg/ml)
C1	44	24.8	51.3
C2	44	24.7	48.8
C3	45	21.7	50.1
C4	46	34.6	45.1
C5	50	22.7	47.7
C6	55	24.7	54.2
C7	56	25.4	40.8
C8	57	31.6	49.5
C9	58	24.7	45.5
C10	58	22.7	43.1
Mean ± SD	51.4±5.8	25.8±4.1	

[a]BMI, body mass index.

Mini-Protean Tetra Cell (Bio-Rad Laboratories) at constant voltage for 30 min at 45 V, and then at 90 V until the dye front reached the gel bottom. Proteins were then trasferred to 0.45 μm PVDF membranes (Milipore, MA) in semi-dry blotter (Hoeffer, Canada) at 0.8 mA/cm^2. Membranes were incubated with PBS-T (phosphate-buffered saline with 0.1% Tween-20) for 2 h. As a primary antibody, mouse anti-RBP4 (Sc-69795, Santa Cruz Biotechnology, CA, USA) diluted 1:500 in PBS-T or rabbit anti-transthyretin (Sigma) diluted 1:1000 was added for 1 h. After thorough washing with PBS-T, secondary horseradish peroxidase-conjugated goat anti-mouse IgG antibody or goat anti-rabbit IgG antibody (both Santa Cruz Biotechnology) diluted 1:10,000 was added for 1 h. Membranes were thoroughly washed in PBS-T and then in PBS. Signal was developed using Western Blotting Luminol Reagent (Santa Cruz Biotechnology) and membranes were exposed to X-ray film (Kodak, CR), developed and scanned. For detection of human IgG as an internal loading control, the membrane were stripped and re-probed with a swine anti-IgG antibody (Sevapharma a.s., Czech Republic) conjugated with HRP diluted 1:10,000.

RBP4 ELISA. The quantitative determination of human retinol-binding protein 4 (RBP4), α-1-antitrypsin and apolipoprotein A4 concentrations in patient and control sera was performed in triplicates using the Quantikine Human RBP4 immunoassay (R&D Systems, MN, USA), human apolipoprotein AIV ELISA Kit (Millipore, MA, USA) and α-1-antitrypsin Clearance ELISA (Immuno Diagnostik AG, Germany) according to the manufacturer's instructions using ELISA Reader Sunrise (Tecan, Austria).

Measurement of plasma vitamin A. Vitamin A serum levels were determined by HPLC method using ClinRep Complete Kit for vitamins A and E in Plasma (Iris technologies international, Germany) on ECOM HPLC according to the manufacturer's instructions.

Statistical analysis. Statistical significances of normalized optical spot density, values from ELISA tests and retinol measurements by HPLC was determined by Student's t-test. Correlation between variables was determined by Correlation Pearson's coefficient using software Statistica (StatSoft Inc., USA).

Results

Patients and controls. The women enrolled in the study were patients diagnosed with EOC (histologically confirmed) and age-matched healthy women. Average age was 53.6±5.3 for patients and 51.4±5.8 for healthy controls. Details are provided in the Tables I and II.

Serum equalization and proteomics. To eliminate potential inter-individual variability, our analysis was performed with

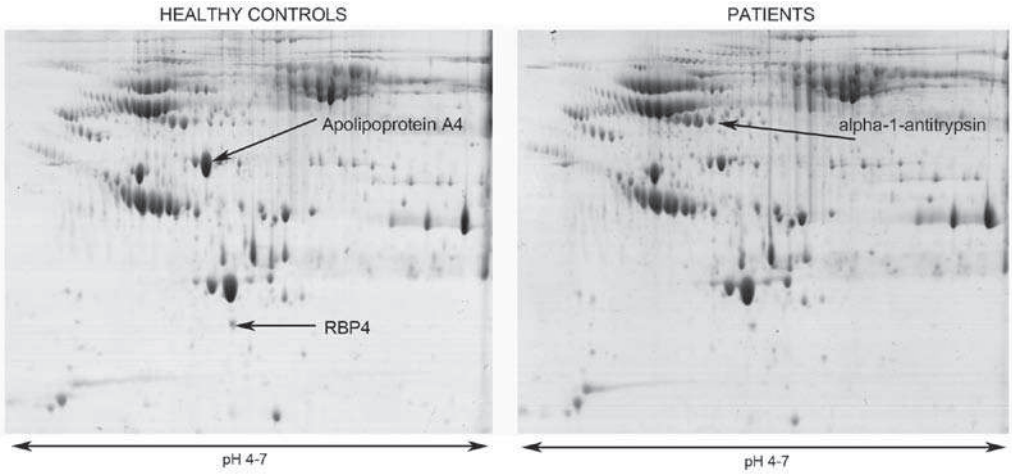

Figure 1. 2-DE analysis of sera after hexapeptide ligand library treatment. 2-DE proteomic analysis of pooled sera from healthy women and EOC patients after ProteoMiner equalization. Twelve 20.5x25-cm gels were analyzed, 6 replicates with pooled patient samples and 6 gels with pooled healthy control samples. Gels were stained, scanned and analyzed by Progenesis PG200/PG220 image analysis software. Three spots of significantly different density between the groups were found and the three proteins were identified by MALDI mass spectrometry using peptide mass fingerprinting (Table III).

Table III. Peptide mass fingerprint identification of proteins with differential concentrations (difference at least 2-fold and statistical significance ($p<0.01$) in sera of EOC patients.

Sequence coverage[a] (%)	Matched peptides	Mascot score[b]	Swiss-Prot access no.[c]	Protein name	Fold-change
Down-regulated in EOC patients					
58	28	335	P06727	Apolipoprotein A-IV	-2.3
57	11	153	P02753	Retinol-binding protein 4	-2.2
Up-regulated in EOC patients					
42	17	115	P01009	α-1-antitrypsin	2.0

[a]Sequence coverage is the number of amino acids spanned by the assigned peptides divided by the sequence length. [b]MASCOT score helps to estimate correctness of the individual hit. It is expressed as -10 x log(P) where P is the probability that the observed match is a random event. [c]SwissProt access no. is the code under which the identified protein is deposited in the SwissProt database.

pooled serum samples from 10 patients diagnosed with EOC (patients) and 10 healthy age-matched women (controls). Later verifications by Western blotting and ELISA were done with individual serum samples.

The dynamic range of individual protein concentrations in serum was reduced or equalized by interaction of serum proteins with of random hexapeptide library immobilized on beads (ProteoMiner) (8). Using the equalized pooled sera we performed classical 2-DE differential proteomic analysis. Equalization of serum samples with hexapeptide ligand library beads was effective, increasing the number of spots detected in 2-DE gels ~1.5 fold compared to untreated sera in a pilot experiment (data not shown).

Twelve 2-DE gels were analyzed (six replicates with pooled patient samples and 6 gels with pooled healthy control samples). On average we detected 410 protein spots per gel upon colloidal Coomassie staining. Quantitative analysis of normalized spot density using Progenesis PG200/PG220 software revealed statistically significant difference [normalized spot volume difference at least 2-fold and statistical significance ($p<0.01$)] between the control and patient groups in 3 spots (Fig. 1). All three proteins present in the spots of differential density were identified by MALDI-TOF mass spectrometry using peptide fingerprint method (Table III). The only up-regulated protein found in sera of ovarian cancer patients has been identified as α-1-antitrypsin. Two proteins with concentrations decreased in patient sera were apolipoprotein A-IV and retinol-binding protein 4 (RBP4).

Retinol binding protein 4 is decreased in EOC patients. α-1-antitrypsin and apolipoprotein A-IV belong among the 40 most abundant plasma proteins, with concentrations 18-40 μmol/l and 3-6 μmol/l, respectively (9). We verified the altered concentrations in these two proteins by ELISA in all individual patient and control serum samples. α-1-antitrypsin was significantly ($p=0.015$) upregulated in patients while apolipoprotein A-IV was markedly downregulated ($p=0.0001$) (Fig. 2). Both proteins were identified by proteomic serum analyses as potential ovarian cancer markers previously (10,11) and we therefore focused our attention to retinol binding protein 4 (RBP4) as the novel observation and the potentially more interesting candidate biomarker (concentration in patient serum decreased 2.2-fold, $p<0.001$).

Since our proteomic analysis was performed with pooled and equalized serum samples, it was necessary to confirm

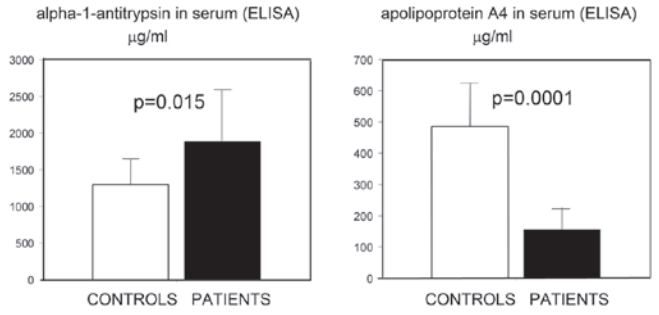

Figure 2. Verification of altered concentrations of α-1-antitrypsin and apolipoprotein A-IV in patient and healthy women sera. Serum concentrations of the proteins were determined in all 10 patient and 10 control serum samples using ELISA kits. α-1-antitrypsin was confirmed to be significantly up-regulated in patients and apolipoprotein A4 was significantly downregulated. Mean values, and statistical significances are shown.

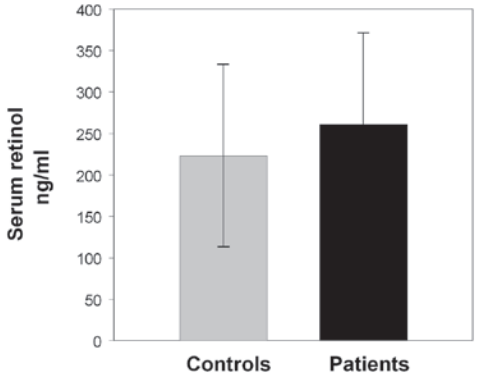

Figure 4. Serum retinol levels in EOC patients and age-matched healthy women. Levels of serum vitamin A (retinol) regulate RBP4 secretion by liver. Decreased retinol levels could affect RBP4 levels in our study. We therefore determined serum retinol levels in all 10 patients and controls by HPLC. Mean values of serum retinol concentrations are shown.

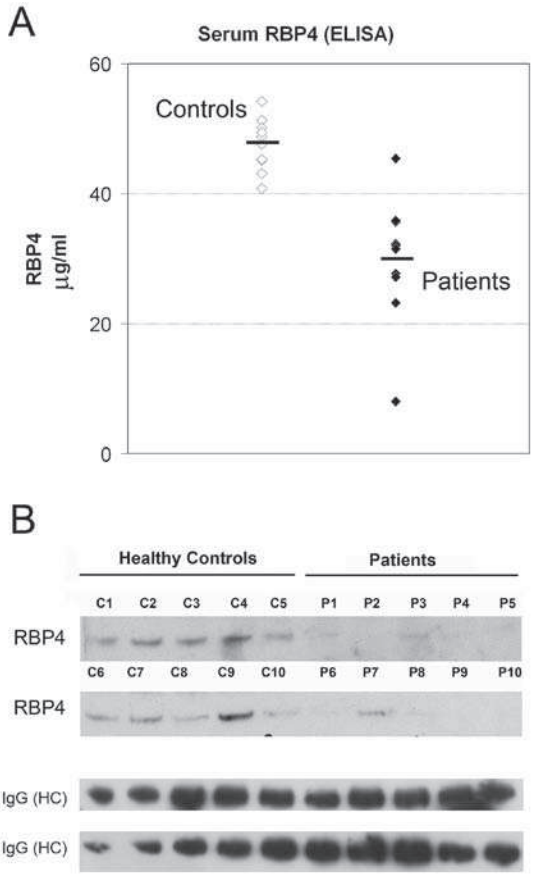

Figure 3. Verification of altered RBP4 concentration. (A) Absolute RBP4 concentrations in serum samples were determined by ELISA. Each measurement represents average value from 3 replicates. Individual serum RBP4 concentrations can be found in Tables I and II. (B) Western blot analysis of RBP4 concentration in individual serum samples was performed. To enable relative comparison between healthy controls and patients five control and five patient samples (10 μg protein each) were run on each gel and processed simultaneously. Membranes were re-probed with anti-human IgG (HC) as an internal standard.

the altered RBP4 abundance in the individual, crude serum samples before the ProteoMiner equalization. To determine also absolute concentrations of RBP4 we used an ELISA test to measure RBP4 in the original set of the all individual non-equalized serum samples from 10 EOC patients and 10 controls. As seen in Fig. 3A, ELISA results confirmed decreased serum concentration of RBP4 in the EOC patients. The average RBP4 concentration in patient serum samples (29.9 μg/ml) was 1.6-fold decreased compared to the control samples (47.7 μg/ml, $p<0.007$). Distribution of the RBP4 concentrations suggests that a threshold exists at 38-40 μg/ml distinguishing healthy age-matched women from most ovarian cancer patients in our cohort. For the individual RBP4 levels see Tables I and II. Serum RBP4 concentrations negatively correlate with ovarian cancer marker CA125 levels in the patient group ($r=-0.715$, $p=0.015$).

To provide additional verification (using different antibodies, than the one used for ELISA) we performed also RBP4 immunodetection using Western blotting with non-equalized sera from all 10 individual patients in the group and the 10 healthy controls (Fig. 3B). The results also confirmed that RBP4 was significantly decreased in patient samples compared to sera from healthy women. Equal sample loading (10 μg per lane) was ensured by careful and repeated determination of protein concentration in samples. Internal standard [total human IgG (HC)] is shown only for rough loading control. Due to high individual variability of serum protein levels, there is currently no reliable and generally accepted internal standard for serum samples (similar to β-actin, GAPDH or tubulin used for tissues).

Serum retinol-binding protein 4 is a 21-kDa lipocalin produced by liver, adipocytes, macrophages and some epithelial cells. It is the principal transport protein for retinol (vitamin A). RBP4 levels in blood are normally maintained within narrow limits with one exception. RBP4 secretion by its main producer, liver, is tightly regulated by availability of retinol levels. In vitamin A deficiency is RBP4 retained in liver, upon retinol repletion RBP4 associates with the vitamin and is secreted into blood (12,13). We therefore tested, whether the decreased concentration RBP4 identified in EOC patients could be attributed to decreased retinol levels. We measured retinol levels in individual serum samples of all 10 individual patients and the 10 healthy controls in our study. As seen in Fig. 4, average serum retinol concentration is comparable

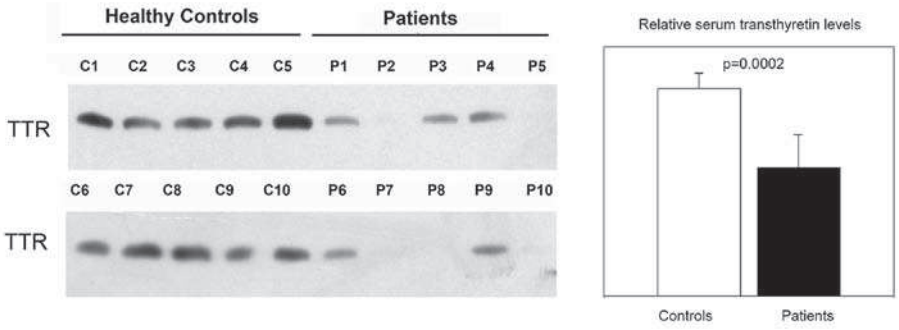

Figure 5. Relative serum transthyretin (TTR) levels in patients and controls. (A) Western blot analysis of TTR concentration in individual serum samples was performed. To enable relative comparison between healthy controls and patients, five control and five patient samples (10 μg protein each) were run on each gel. (B) Densitometric analysis of the TTR bands from the Western blot analysis.

between the patients and healthy women. Hence, we concluded that the decrease in RBP4 concentration in EOC patients is independent on serum vitamin A levels.

RBP4 is a relatively small protein and to avoid glomerular filtration it associates with transthyretin (TTR) (12). Interestingly, transthyretin has also been identified as down-regulated in blood of ovarian cancer patients and considered as a potential biomarker (14-16). We determined relative serum transthyretin levels in our group of patients and control women and confirmed its down-regulation in our EOC patients (1.6-fold change, p=0.002) (Fig. 5). There was no marked correlation of TTR levels with RBP4.

Discussion

RBP4 is secreted by liver, adipose tissue and some epithelia including ovarian and serves as an important transporter of retinol. Retinoids play an important role in fundamental aspects of human physiology such as hematopoiesis, reproduction and cell proliferation. Anti-cancer effect of retinoids was reported long ago (17). Alterations of vitamin A and retinoid homeostasis are found in many tumors. Defects in expression of retinol metabolism genes, namely its crucial components cellular retinol-binding protein 1 (CRBP1) and RBP4, have been previously reported in ovarian cancer and connected with the oncogenic process in a rat model of ovarian cancer (18,19). Moreover, defective conversion of retinol to retinoic acid has been demonstrated in ovarian carcinoma cell lines (20).

The observed decrease in concentration of RBP4 in sera of EOC patients identified here may be theoretically attributed to decreased RBP4 production by ovary. Regrettably, we do not know how much RBP4 ovary contributes to the total circulating RBP4 pool. Considering the fact, that liver and adipose tissue are believed to be the main producers of the circulating RBP4, it remains to be determined whether decreased production of RBP4 in ovary may be reflected in total circulating RBP4 levels in EOC patients.

Alternative hypothesis which considers a systemic process and the liver and/or adipose tissue as a source of the altered RBP4 levels can also be proposed. We demonstrated that levels of retinol are comparable between patients and controls. Decreased levels of RBP4 in patients therefore can not be explained by different retinol availability between the groups. In addition to its role as a vitamin A transporter RBP4 attracted wide attention as a molecule involved in insulin resistance in mice (21) and as a protein elevated in serum of patients with impaired glucose tolerance and type 2 diabetes (insulin resistance) (22). These observations were followed by many other reports, in the wider metabolic area related to insulin and glucose and fat metabolism. RBP4 has thus been shown to be elevated in obese patients with polycystic ovary syndrome (disease associated with insulin resistance) (23) and in patients with renal dysfunction and cardiac disease in type 2 diabetes patients (24). To exclude a potential influence of such a cancer-unrelated factor we verified anamnesis of our healthy controls and patients. None of the women involved in our study had history, or evidence of type 2 diabetes.

What could then be the connection between RBP4 energy metabolism and ovarian cancer? Is it a tumor-specific response or rather a reflection of general metabolic changes taking place in cancer patients? Controversy exists, whether there is a general correlation between RBP4 levels and body-mass index in otherwise healthy women. Whereas some investigators showed lower serum RBP4 levels in healthy lean women compared to obese (22), others demonstrated that there is no such a correlation (25). However, since levels of RBP4 have been reported to decrease in morbidly obese patients after weight loss due to gastric banding surgery (26), we tested a hypothesis that the decreased levels of RBP4 observed in our patient group could be attributed to cancer-induced cachexia. However, comparison of body-mass indexes (BMI) between our patients and healthy controls showed, that there is only a marginal and statistically insignificant (p=0.126) BMI decrease in our group of EOC patients and there is no correlation of serum RBP4 concentration with BMI (r=-0.001, p=0.99). This observation therefore does not support the hypothesis that the reduced RBP4 level in blood of EOC patients is caused by cancer-related decrease in BMI. However, we are aware, that the decrease in serum RBP4 in EOC patients may be an early sign of cancer-triggered nutritional changes before they become apparent by weight loss. Such a marker would be of wider clinical interest because cancer-induced cachexia indeed complicates therapy and has been implicated in up to 20% of cancer-related deaths (27,28).

We identified significantly decreased RBP4 concentrations in sera of EOC patients. We excluded influence of diabetes, serum retinoid levels and BMI as potential causes of the decreased RBP4 levels and we therefore believe that the phenomenon is cancer related. We are fully aware that the low

number of patients enrolled in our proteomic discovery phase of the study must be compensated for in future verification process using large cohorts of patients and controls stratified by stage/grade and other factors.

The decreased RBP4 concentration in sera of EOC patients is either directly connected with altered retinoid metabolism and RBP4 production in ovary or it is a reflection of a more general process involving energy metabolism or other systemic changes. In both cases, the cancer-related information represented by RBP4 serum levels, is of clinical interest and should be evaluated as a potential biomarker.

So far, none of the candidate molecules identified by proteomic analyses of ovarian cancer (10, 11, 14 and many others) have been implemented into clinical practice as a single diagnostic biomarker. However, as demonstrated by recent development, combined informative power of several weak biomarkers can be valuable in clinical decision-making in assessment of ovarian tumors (29). We believe that RBP4 can increase diagnostic performance of such a multivariate biomarker panel in future.

Acknowledgements

This study was supported by grants from the Ministry of Health CR, (IGA MZCR NT12248-5 to J.Z. and NS10300-3 and UHKT No. 023736 to J.P.), from the Ministry of Education, Youth and Sports, CR (VZ 0021620806 to J.Z., LC06044 to J.P. and SVV-2011-262507 to L.L.), from the Grant agency of the Czech Republic (305/09/1390 to J.P.) and Grant agency of the Charles University (GAUK 251180 111210 to Jana Pospislova). Authors would like to thank Milada Kostirova for plasma vitamin A measurements and Ondrej Vit for his assistance with western blotting. Special thanks to Mrtva Ryba.

References

1. Heintz APM, Odicino F, Maisonneuve P, *et al*: Carcinoma of the ovary. FIGO 26th Annual Report on the Results of Treatment in Gynaecological Cancer. Int J Gynaecol Obstet 95: S161-S192, 2006.
2. Skirnisdottir I and Sorbe B: Prognosti factor for surgical outcome and survival in 447 women treated for advanced (FIGO-stages III-IV) epithelial ovarian carcinoma. Int J Oncol 30: 727-734, 2007.
3. Moore RG, MacLaughlan S and Bast RC Jr: Current state of biomarker development for clinical application in epithelial ovarian cancer. Gynecol Oncol 116: 240-245, 2010.
4. Husseinzadeh N: Status of tumor markers in epithelial ovarian cancer has there been any progress? A review. Gynecol Oncol 120: 152-157, 2011.
5. Narasimhan K, Changqing Z and Choolani M: Ovarian cancer proteomics: Many technologies one goal. Proteomics Clin Appl 2: 195-218, 2008.
6. Anderson NL and Anderson NG: The human plasma proteome: history, character, and diagnostic prospects. Mol Cell Proteomics 1: 845-867, 2002.
7. Pernemalm M, Lewensohn R and Lehtio J: Affinity prefractionation for MS-based plasma proteomics. Proteomics 9: 1420-1427, 2009.
8. Boschetti E and Righetti PG: The ProteoMiner in the proteomic arena: a non-depleting tool for discovering low-abundance species. J Proteomics 71: 255-264, 2008.
9. Hortin GL, Sviridov D and Anderson NL: High-abundance polypeptides of the human plasma proteome comprising the top 4 logs of polypeptide abundance. Clin Chem 54: 1608-1616, 2008.
10. Chen Y, Lim BK, Peh SC, Abdul-Rahman PS and Hashim OH: Profiling of serum and tissue high abundance acute-phase proteins of patients with epithelial and germ line ovarian carcinoma. Proteome Sci 6: 20, 2008.
11. Dieplinger H, Ankerst DP, Burges A, Lenhard M, *et al*: Afamin and apolipoprotein A-IV: novel protein markers for ovarian cancer. Cancer Epidemiol Biomarkers Prev 18: 1127-1133, 2009.
12. Muto Y, Smith JE, Milch PO and Goodman DS: Regulation of retinol-binding protein metabolism by vitamin A status in the rat. J Biol Chem 247: 2542-2550, 1972.
13. Peterson PA, Rask L, Ostberg L, Anderson L, Kamwendo F and Pertoft H: Studies on the transport and cellular distribution of vitamin A in normal and vitamin A-deficient rats with special reference to the vitamin A-binding plasma protein. J Biol Chem 248: 4009-4022, 1973.
14. Zhang Z, Bast RC Jr, Yu Y, *et al*: Three biomarkers identified from serum proteomic analysis for the detection of early stage ovarian cancer. Cancer Res 64: 5882-5890, 2004.
15. Kozak KR, Su F, Whitelegge JP, Faull K, Reddy S and Farias-Eisner R: Characterization of serum biomarkers for detection of early stage ovarian cancer. Proteomics 5: 4589-4596, 2005.
16. Mählck CG and Grankvist K: Plasma prealbumin in women with epithelial ovarian carcinoma. Gynecol Obstet Invest 37: 135-140, 1994.
17. Clarke N, Germain P, Altucci L and Gronemeyer H: Retinoids: potential in cancer prevention and therapy. Expert Rev Mol Med 6: 1-23, 2004.
18. Roberts D, Williams SJ, Cvetkovic D, Weinstein JK, Godwin AK, Johnson SW and Hamilton TC: Decreased expression of retinol-binding proteins is associated with malignant transformation of the ovarian surface epithelium. DNA Cell Biol 21: 11-19, 2002.
19. Cvetković D, Williams SJ and Hamilton TC: Loss of cellular retinol-binding protein 1 gene expression in microdissected human ovarian cancer. Clin Cancer Res 9: 1013-1020, 2003.
20. Williams SJ, Cvetkovic D and Hamilton TC: Vitamin A metabolism is impaired in human ovarian cancer. Gynecol Oncol 112: 637-645, 2009.
21. Yang Q, Graham TE, Mody N, *et al*: Serum retinol binding protein 4 contributes to insulin resistance in obesity and type 2 diabetes. Nature 436: 356-362, 2005.
22. Graham TE, Yang Q, Blüher M, *et al*: Retinol-binding protein 4 and insulin resistance in lean, obese, and diabetic subjects. N Engl J Med 354: 2552-2563, 2006.
23. Tan BK, Chen J, Lehnert H, Kennedy R and Randeva HS: Raised serum, adipocyte, and adipose tissue retinol-binding protein 4 in overweight women with polycystic ovary syndrome: effects of gonadal and adrenal steroids. J Clin Endocrinol Metab 92: 2764-2772, 2007.
24. Cabré A, Lázaro I, Girona J, *et al*: Retinol-binding protein 4 as a plasma biomarker of renal dysfunction and cardiovascular disease in type 2 diabetes. J Intern Med 262: 496-503, 2007.
25. Kowalska I, Straczkowski M, Adamska A, Nikolajuk A, Karczewska-Kupczewska M, Otziomek E and Gorska M: Serum retinol binding protein 4 is related to insulin resistance and nonoxidative glucose metabolism in lean and obese women with normal glucose tolerance. J Clin Endocrinol Metab 93: 2786-2789, 2008.
26. Haider DG, Schindler K, Prager G, Bohdjalian A, Luger A, Wolzt M and Ludvik B: Serum retinol-binding protein 4 is reduced after weight loss in morbidly obese subjects. J Clin Endocrinol Metab 92: 1168-1171, 2007.
27. Inui A: Cancer anorexia-cachexia syndrome: current issues in research and management. CA Cancer J Clin 52: 72-91, 2002.
28. MacDonald N, Easson AM, Mazurak VC, Dunn GP and Baracos VE: Understanding and managing cancer cachexia. J Am Coll Surg 197: 143-161, 2003.
29. Ueland FR, Desimone CP, Seamon LG, *et al*: Effectiveness of a multivariate index assay in the preoperative assessment of ovarian tumors. Obstet Gynecol 117: 1289-1297, 2011.

Klanova et al. Molecular Cancer 2014, 13:159
http://www.molecular-cancer.com/content/13/1/159

MOLECULAR CANCER

RESEARCH Open Access

Downregulation of deoxycytidine kinase in cytarabine-resistant mantle cell lymphoma cells confers cross-resistance to nucleoside analogs gemcitabine, fludarabine and cladribine, but not to other classes of anti-lymphoma agents

Magdalena Klanova[1,2], Lucie Lorkova[1], Ondrej Vit[1], Bokang Maswabi[1], Jan Molinsky[1,2], Jana Pospisilova[1], Petra Vockova[1,2], Cory Mavis[3], Lucie Lateckova[1,2], Vojtech Kulvait[1], Dana Vejmelkova[2], Radek Jaksa[3], Francisco Hernandez[4], Marek Trneny[2], Martin Vokurka[1], Jiri Petrak[1,5†] and Pavel Klener Jr[1,2*†]

Abstract

Background: Mantle cell lymphoma (MCL) is an aggressive type of B-cell non-Hodgkin lymphoma associated with poor prognosis. Implementation of high-dose cytarabine (araC) into induction therapy became standard-of-care for all newly diagnosed younger MCL patients. However, many patients relapse even after araC-based regimen. Molecular mechanisms responsible for araC resistance in MCL are unknown and optimal treatment strategy for relapsed/refractory MCL patients remains elusive.

Methods: Five araC-resistant (R) clones were derived by long-term culture of five MCL cell lines (CTRL) with increasing doses of araC up to 50 microM. Illumina BeadChip and 2-DE proteomic analysis were used to identify gene and protein expression changes associated with araC resistance in MCL. *In vitro* cytotoxicity assays and experimental therapy of MCL xenografts in immunodeficient mice were used to analyze their relative responsiveness to a set of clinically used anti-MCL drugs. Primary MCL samples were obtained from patients at diagnosis and after failure of araC-based therapies.

Results: Marked downregulation of deoxycytidine-kinase (DCK) mRNA and protein expression was identified as the single most important molecular event associated with araC-resistance in all tested MCL cell lines and in 50% primary MCL samples. All R clones were highly (20-1000x) cross-resistant to all tested nucleoside analogs including gemcitabine, fludarabine and cladribine. *In vitro* sensitivity of R clones to other classes of clinically used anti-MCL agents including genotoxic drugs (cisplatin, doxorubicin, bendamustine) and targeted agents (bortezomib, temsirolimus, rituximab) remained unaffected, or was even increased (ibrutinib). Experimental therapy of immunodeficient mice confirmed the anticipated loss of anti-tumor activity (as determined by overall survival) of the nucleoside analogs gemcitabine and fludarabine in mice transplanted with R clone compared to mice transplanted with CTRL cells, while the anti-tumor activity of cisplatin, temsirolimus, bortezomib, bendamustine, cyclophosphamide and rituximab remained comparable between the two cohorts.

(Continued on next page)

* Correspondence: pavel.klener@gmail.com
†Equal contributors
[1]Institute of Pathological Physiology, Charles University in Prague, First Faculty of Medicine, Prague, Czech Republic
[2]First Department of Medicine - Department of Hematology, General University Hospital and Charles University in Prague, Prague, Czech Republic
Full list of author information is available at the end of the article

(Continued from previous page)

Conclusions: Acquired resistance of MCL cells to araC is associated with downregulation of DCK, enzyme of the nucleotide salvage pathway responsible for the first phosphorylation (=activation) of most nucleoside analogs used in anti-cancer therapy. The data suggest that nucleoside analogs should not be used in the therapy of MCL patients, who relapse after failure of araC-based therapies.

Keywords: Mantle cell lymphoma (MCL), Cytarabine, Drug resistance, Nucleotide salvage pathway, Proteomics, Mass spectrometry

Background

Mantle cell lymphoma (MCL) is an aggressive type of B-cell non-Hodgkin lymphoma (NHL) associated with poor prognosis [1,2]. In recent years several studies brought evidence that implementation of high-dose cytarabine (araC) into induction therapy, e.g. by sequential chemotherapy by R(ituximab)-CHOP and R-DHAP regimens, induced higher response rate and prolonged progression-free survival compared to R-CHOP-only [3-5]. Based on these results, implementation of araC into induction therapy became standard of care for all newly diagnosed younger MCL patients. Despite considerable improvement, however, most high-risk MCL patients relapse even after araC-based first-line regimen. Prognosis of relapsed/refractory (RR) MCL is dismal. Currently, there is no second-line standard-of-care for RR-MCL [6]. Available treatment approaches for RR-MCL include cisplatin, fludarabine, cladribine, gemcitabine, temsirolimus, bortezomib, bendamustine, lenalidomide and ibrutinib-based regimen [7-16].

AraC belongs among the backbone anti-leukemia agents [17]. Both, "standard dose" araC (100-200 mg/m2 continuous i.v. infusion for 7 days), and "high dose" araC (HDAC, 2-3 g/m2, 2–4 i.v. three hour administrations every 12–24 hours) have been widely used in the therapy of acute myelogenous leukemia (AML), as well as in salvage regimen for relapsed B-NHL [18,19]. As mentioned above araC appears particularly effective component of multi-agent aggressive immunochemoterapy regimen used in younger MCL patients.

AraC is a prodrug, which must be 1. transported into the cell, and 2. within the cell converted into an active drug by phosphorylation by specific phosphokinases of the nucleotide salvage pathway [20]. During "standard dose" cytarabine administration araC is transported into the cell by means of specific transporters, primarily via hENT1/SLC29A1 [21]. During high-dose cytarabine administration araC also diffuses across plasma membrane independent of the specific transporters [22]. The rate-limiting enzyme of the nucleotide salvage pathway is deoxycytidine-kinase (DCK), which catalyzes the first phosphorylation of araC into araCMP. AraCMP is retained in the cell and undergoes two additional consecutive phosporylations before it can be incorporated into DNA.

The molecular mechanisms of araC resistance in MCL are unknown. Resistance to araC in myeloid leukemia cells was repeatedly associated with altered expression of genes involved in nucleotide salvage pathway, including downregulation of DCK, or upregulation of key araC-inactivating enzymes, namely cytidine-deaminase (CDA) or cytoplasmic 5′nucleotidase (NT5C2) [20-25].

In this study we derived araC-resistant MCL cells, studied their sensitivity to a battery of anti-cancer drugs and elucidated the molecular mechanism responsible for araC resistance in MCL.

Results

Establishment and characterization of araC-resistant MCL clones (R clones)

Five araC-resistant MCL clones (=R clones) were established by long-term culture of five cytarabine-sensitive MCL cell lines (JEKO-1, MINO, REC-1, HBL-2 and GRANTA-519, =CTRL cell lines) in the presence of increasing doses of araC (up to 50 μM, comparable with plasma concentration reached in patients treated with high-dose araC) [26]. Resistance of R clones to araC was confirmed *in vitro* by proliferation assays (Figure 1). The R clones tolerated at least 125-1000-fold higher concentrations of araC compared to CTRL cells (Figure 1).

Gene expression profiling of R clones revealed downregulation of deoxycytidine-kinase (DCK)

To identify gene and protein expression changes associated with araC resistance in MCL we performed parallel transcriptome profiling and proteomic analysis of R clones compared to CTRL cell lines. Transcriptomic analysis was performed for each of the 5 MCL cell lines and their respective R clones in biological duplicates using Illumina BeadChips. The filtered groups of genes with fold change at least ± 1.5-fold and adjusted p value < 0.05 were annotated and arranged into biologically relevant categories using The Database for Annotation, Visualization and Integrated Discovery (DAVID, Additional file 1: Figure S1). Based on Gene Ontology (GO) terms, the downregulated genes were involved in *ribosome structure and function*, *cell cycle*, *RNA degradation*, *antigen processing and presentation*, *purine metabolism* and *pyrimidine metabolism*

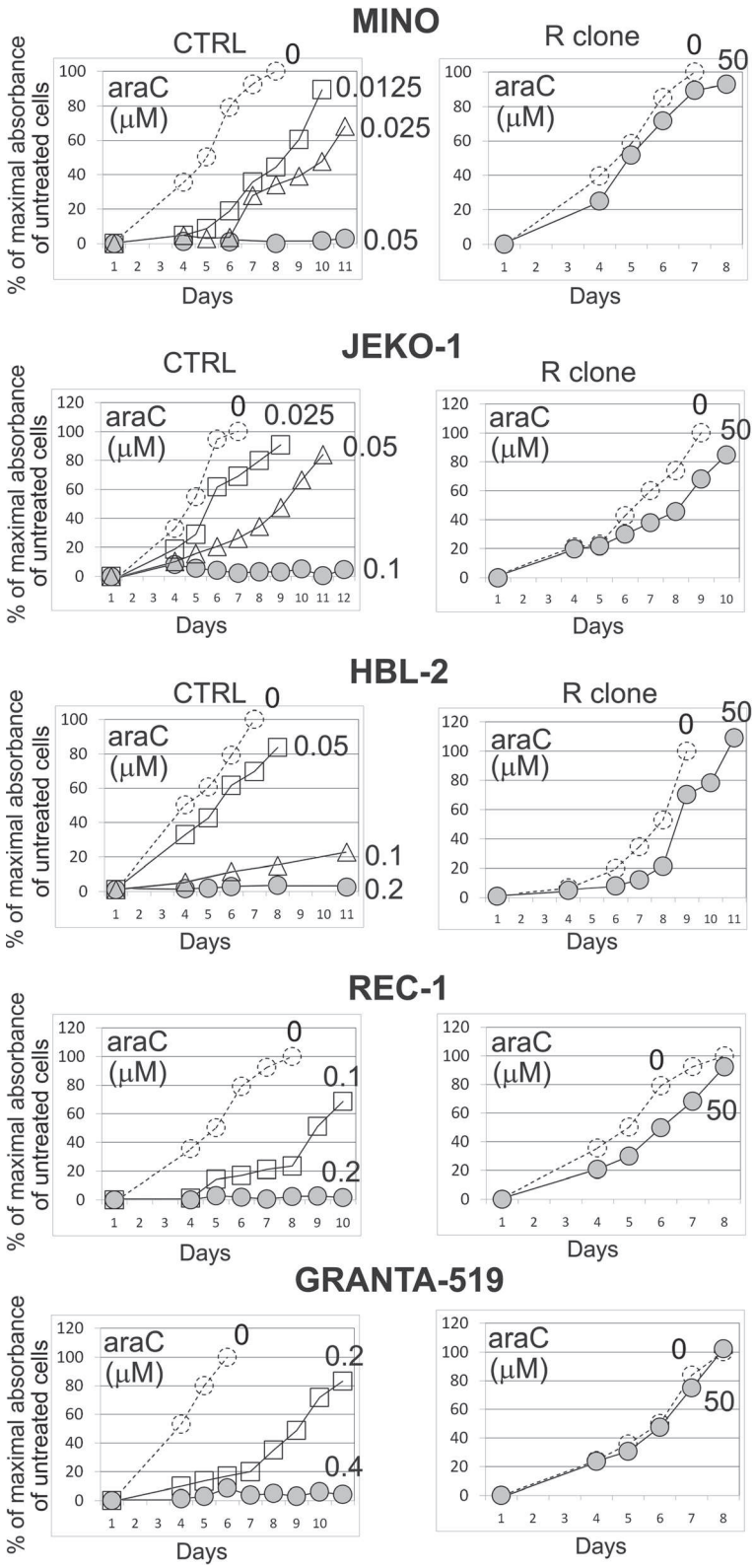

Figure 1 R clones are resistant to 50 μM cytarabine. WST-8 cell proliferation assay of 5 MCL cell lines (CTRL) and 5 R clones was carried out as described in Methods. While the lethal dose of cytarabine for CTRL cells ranged from 0.05 to 0.4 μM, proliferation rate of R clones in 50 μM araC was virtually unaffected. Representative example of two independent experiments is shown. Standard deviations were < 5% for all measurements.

(Additional file 1: Figure S1A). Among the most upregulated gene groups belonged those involved in *graft-vs-host disease*, *alograft rejection*, *B-cell receptor signaling*, *cell adhesion molecules*, *chemokine signaling pathway* and *Toll-like receptor signaling* (Additional file 1: Figure S1B). The only gene consistently differentially expressed across all 5 MCL cell lines was DCK, which was markedly downregulated in all R clones. Other genes differentially expressed in more than one MCL cell line are shown in Additional file 2: Table S1. Proteomic analysis using 2-DE was applied to Mino R subclone compared to Mino CTRL cell line, and revealed differential expression of several proteins, among them almost 5-fold downregulation of DCK in the Mino R subclone was the most apparent (Figure 2, Tables 1 and 2). Downregulation of DCK protein (the rate-limiting enzyme of the nucleotide salvage pathway, which catalyzes the first phosphorylation of araC and other nuclosides into their respective monophosphates) was confirmed by western blotting in all five R clones (Figure 3). DCK expression seemed to be fully abrogated in four R clones (as there was no detectable DCK) and several-fold downregulated in one R clone compared to the CTRL cells.

AraC-resistant clones are cross-resistant to nucleoside analogs, but remain sensitive to other classes of anti-lymphoma agents

To identify optimal treatment strategy for araC-resistant MCL we determined sensitivity (or eventual cross-resistance) of all 5 R clones in a battery of cellular toxicity tests. We exposed R clones and CTRL cells to a panel of clinically used anti-MCL agents in various concentrations and measured their effect on cell proliferation rate. The tested agents included both, classical genotoxic cytostatics and novel targeted drugs. The panel included alkylating agents cisplatin, doxorubicin and bendamustine, nucleoside analogs gemcitabine, cladribine and fludarbine, and targeted drugs bortezomib (proteasome inhibitor), temsirolimus (mTOR inhibitor) and ibrutinib (Bruton tyrosine-kinase (BTK) inhibitor). All five R clones (resistant to a pyrimidine analog cytarabine) showed cross-resistance not only to another pyrimidine analog gemcitabine (up to 3125-fold), but also to purine nucleoside analogs fludarabine and cladribine (approx. 12.5-500-fold, see Figure 4A,B). Sensitivity of the resistant R clones to other classes of anti-lymphoma agents (i.e. other than nucleoside analogs) remained comparable to the respective CTRL cells (Figure 4C,D), with the exception of ibrutinib. The BTK inhibitor ibrutinib proved to be significantly more cytotoxic to R clones compared to CTRL cells *in vitro* (see Figure 4C,D, Additional file 3: Figure S2). R clones also retained *in vitro* sensitivity to anti-CD20 monoclonal antibody rituximab comparable to CTRL cells as determined by ^{51}Cr release assay, which is standardly used to evaluate antibody-dependent cytotoxicity (ADCC) and complement-mediated cytotoxicity (CMC) of therapeutic monoclonal antibodies (Figure 5).

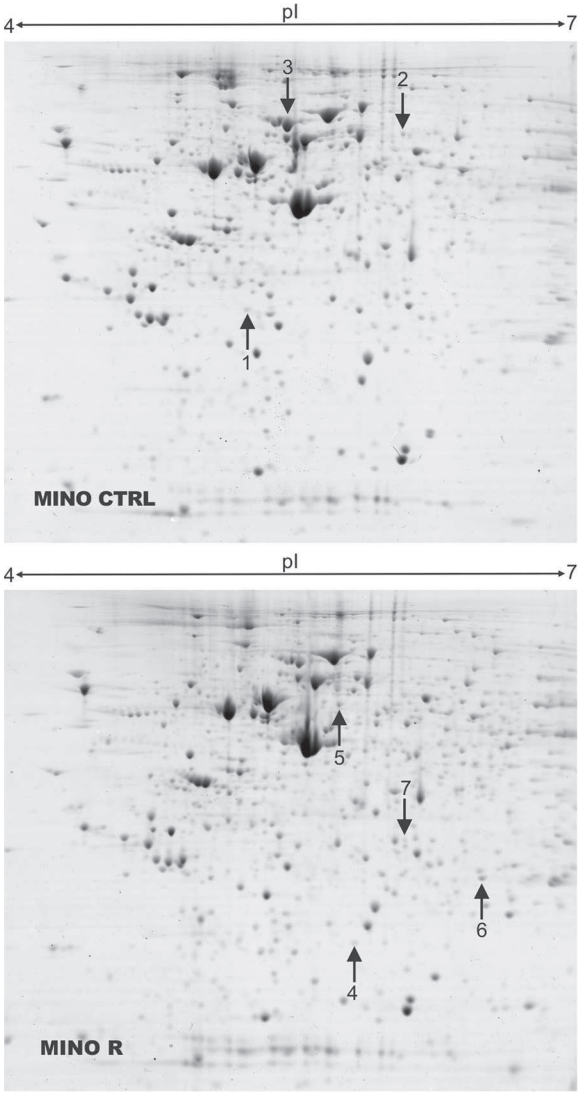

Figure 2 Proteomic analysis of MINO R vs MINO CTRL cells. Two-dimensional electrophoresis of cells MINO R cell versus MINO CTRL cells was performed on 24 cm gel strips, pH 4.0-7.0, 10% SDS-PAGE. Proteins were stained with Coomassie Brilliant Blue. Differentially expressed proteins are indicated by numbered arrows, spots 1–3 indicate proteins significantly downregulated in MINO R cells, and spots 4–7 indicate proteins upregulated in MINO R cells.

Experimental therapy with fludarabine and gemcitabine is ineffective in mice xenografted with araC-resistant clones

The *in vitro* tests of cellular toxicity provided important information on direct cellular effects of the tested drugs to the resistant cells. However, *in vitro* assays do not take into account important systemic pharmacokinetic

Table 1 List of proteins differentially expressed in MINO R cells identified by 2-DE

Spot no.	Accession	Protein name	Fold change	Mascot score	Sequence cov. (%)	Mr
Proteins downregulated in MINO R cells						
1	P27707	Deoxycytidine kinase	−4.6	44*	16	30841
2	Q99829	Copine-1	−4.3	102	17	59649
3	P13796	Plastin-2	−2	453	65	70814
Proteins upregulated in MINO R cells						
4	P07741	Adenine phosphoribosyltransferase	5	70	40	19766
5	P68363	Tubulin alpha-1B chain	5	169	32	50804
6	P04792	Heat shock protein beta-1	2/3	73	32	22826
7	P31937	3-Hydroxyisobutyrate Dehydrogenase, Mitochondrial	2/1	43*	8	35712

*Identity of proteins with low Mascot Score was verified by MS/MS (see Table 2).
Included are the proteins with difference in expression at least 2-fold and statistical significance of the change $p < 0.05$. Swiss-Prot no. is the code under which the identified protein is deposited in the Swiss-Prot database. Mascot score helps to estimate the correctness of the individual hit. It is expressed as $-10 \times \log(P)$ where P is the probability that the observed match is a random event. Sequence coverage is the number of amino acids spanned by the assigned peptides divided by the sequence length.

and pharmacodynamic variables, which can have large impact on the drug efficacy *in vivo*. In addition, some anti-MCL agents cannot be properly tested *in vitro*, because their mechanism of antitumor activity directly or indirectly depends on the *in vivo* context, e.g. activation of a prodrug cyclophosphamide in the liver microsome, cooperation of a monoclonal antibody rituximab with complement and cells of the immune system, or antiangiogenic component of temsirolimus activity. Therefore, we used a mouse xenograft model (NOD.Cg-*Prkdc*^{scid} *Il2rg*^{tm1Wjl}/SzJ mice) of MCL to simulate *in vivo* treatment of araC-sensitive and araC-resistant disease. Intravenous injection of 1 million JEKO-1 MCL cells leads to demise of the xenografted animals due to disseminated lymphoma with median overall survival of approx. 38 days. Experimental therapy of JEKO-1-xenografted immunodeficient mice with single-agent fludarabine and gemcitabine confirmed total loss of anti-tumor activity of purine analog fludarabine and pyrimidine analog gemcitabine (measured as overall survival of experimental animals) in mice transplanted with cytarabine-resistant JEKO-1 R clone compared to mice transplanted with cytarabine-sensitive JEKO-1 CTRL cells (Figure 6). Antitumor activity of cisplatin, temsirolimus, bendamustine, bortezomib, cyclophosphamide and rituximab remained comparable between JEKO-1 R clone and JEKO-1 CTRL-xenografted mice in agreement with the *in vitro* tests (Figure 6).

Analysis of primary MCL samples confirmed that downregulation of DCK is frequently associated with failure of high-dose araC-based treatments

Eight and two primary MCL samples obtained from patients at diagnosis (D1-D8) and at lymphoma relapse after failure of high-dose araC-based treatments (R1-R8) were analyzed by real-time RT-PCR and western blotting, respectively (Table 3, Figure 7A). In four cases downregulation of DCK gene expression was observed in R compared to D samples (difference in ΔCT (DCK-GAPDH) between R and D samples was > 1 cycle), while in four cases no change was observed (difference in ΔCT < 1 cycle) (Table 3). Western blotting analysis of the sample R2 compared to D2 revealed marked downregulation of protein DCK thereby confirming the gene expression results (i.e. 4-fold decrease in total DCK mRNA after araC-based therapy). Interestingly, protein DCK in the sample R6 compared to D6 was also moderately downregulated despite its gene expression remained virtually unchanged (Figure 7A, Table 3). In addition to the analysis of MCL samples obtained from the relapsed patients, paired primary cells isolated from two MCL patients (samples D9/R9, and D10/R10) refractory to araC were subject to analysis of gene and protein expression, and determination of their *ex vivo* sensitivity to nucleoside analogs (Figure 7B,C). The samples were obtained before araC administration (D9, D10), and 14 days after araC administration (R9, R10). Downregulation of both gene

Table 2 Identity of differentially expressed proteins with low mascot score confirmed by MS/MS

Spot no.	Accession	Protein name	Peptide sequence	Score
1	P27707	Deoxycytidine kinase	LKDAEKPVLFFER, QLCEDWEVVPEPVAR	41, 46
7	P31937	3-Hydroxyisobutyrate Dehydrogenase, Mitochondrial	DFSSVFQFLREEETF (C-term), SPILLGSLAHQIYR	49, 28

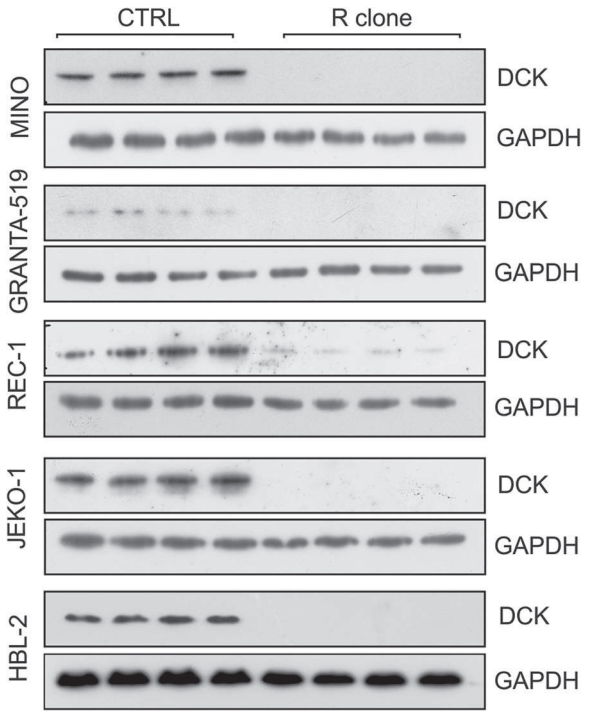

Figure 3 Western blot analysis confirms marked downregulation of protein DCK in all R clones. Relative expression of deoxycytine kinase (DCK) in all five R and CTRL clones. Quadruplicate cell lysates were separated on 12% SDS-PAGE minigels. Proteins were then transferred onto PVDF membranes, blocked and probed with anti-DCK antibody. Anti-GAPDH antibody was used as the loading control.

and protein DCK expression was confirmed in R9 compared to D9 cells (Figure 7B). Sensitivity of R9 cells to araC, fludarabine and gemcitabine was significantly suppressed compared to D9 cells (Figure 7C). Both gene expression and protein expression of R10 compared to D10 sample remained unchanged (Figure 7B). Interestingly, susceptibility of R10 cells compared to D10 cells to undergo apoptosis after their *ex vivo* exposure to araC was increased despite the fact that R10 cells were isolated after administration of four cycles of high-dose araC (Figure 7C).

Discussion

In this study we analyzed molecular mechanisms of araC resistance in five MCL cell lines and ten paired primary MCL samples obtained before and after araC-based therapies. In addition, we tested optimal treatment strategies for cytarabine-resistant MCL. On molecular level we identified marked and principal downregulation of DCK, the rate-limiting enzyme of nucleotide salvage pathway, in all 5 cytarabine-resistant MCL clones, and in 50% primary MCL samples obtained from patients, who progressed on or relapsed after araC-based treatments. In 50% primary MCL samples, no change of DCK expression was observed at time of lymphoma relapse or progression. Importantly, no upregulation of DCK was observed in any of the analyzed post-treatment samples. Although the analysis of the primary MCL samples indicate that the mechanisms responsible for araC resistance *in vivo* are more complex than those observed *in vitro*, it must be emphasized that downregulation of gene and protein DCK was indeed confirmed in a substantial part of the patients' post-treatment samples (Table 3, Figure 7A,B). Interestingly, in one of the two MCL patients primary resistant to araC, no change of DCK expression was observed with slightly increased *ex vivo* sensitivity of post-treatment MCL cells to araC (Figure 7B,C). This observation could be explained by existence of araC-resistant stem cell-like MCL cells that would reside in the niches in lymph nodes (and/or bone marrow) and produce partially araC-sensitive MCL cells mobilized in the peripheral blood. In such a case, elimination of the mobilized MCL cells, but persistence of the stem cell-like MCL compartment, would lead to stable disease, and eventual lymphoma progression (which was the actual course of the disease observed in this patient).

DCK catalyzes the first phosphorylation (=activation necessary for their cytotoxic activity) not only of araC into araCMP, but also of most nucleoside analogs (both pyrimidine and purine-derived) commonly used in anti-cancer therapy. Using DAVID bioinformatic analyzer *purine/pyrimidine metabolism*, and *B-cell receptor signaling* were among the functional cathegories associated with the most downregulated and upregulated genes, respectively. In accordance with these results we subsequently showed that all R clones were cross-resistant to both pyrimidine analog gemcitabine, and to purine analogs fludarabine and cladribine (all of which are activated by DCK). Sensitivity of R clones to other types of anti-cancer molecules including genotoxic cytostatics (cisplatin, doxorubicin, bendamustine), targeted drugs (temsirolimus, bortezomib) or biological agents (monoclonal anti-CD20 antibody rituximab) remained unaffected, or was even augmented in the case of BTK inhibitor ibrutinib. The reason, why ibrutinib more effectively eliminated araC-resistant MCL cells remained elusive, but might be at least partially explained by the observed upregulation of B-cell receptor signaling in R clones compared to CTRL cells (Additional file 1: Figure S1).

The results of our *in vitro* and *in vivo* tests combined with the observed decreased expression of DCK in all araC-resistant MCL clones and in 50% post-treatment primary MCL samples suggest that the resistance of MCL cells to high-dose araC is caused by suppressed araC activation by DCK due to markedly decreased DCK expression. DCK has low substrate preference and phosphorylates both, purines and pyrimidines, including synthetic analogs cytarabine, fludarabine, gemcitabine and cladribine [27-29]. The fact that above-mentioned nucleoside analogs are

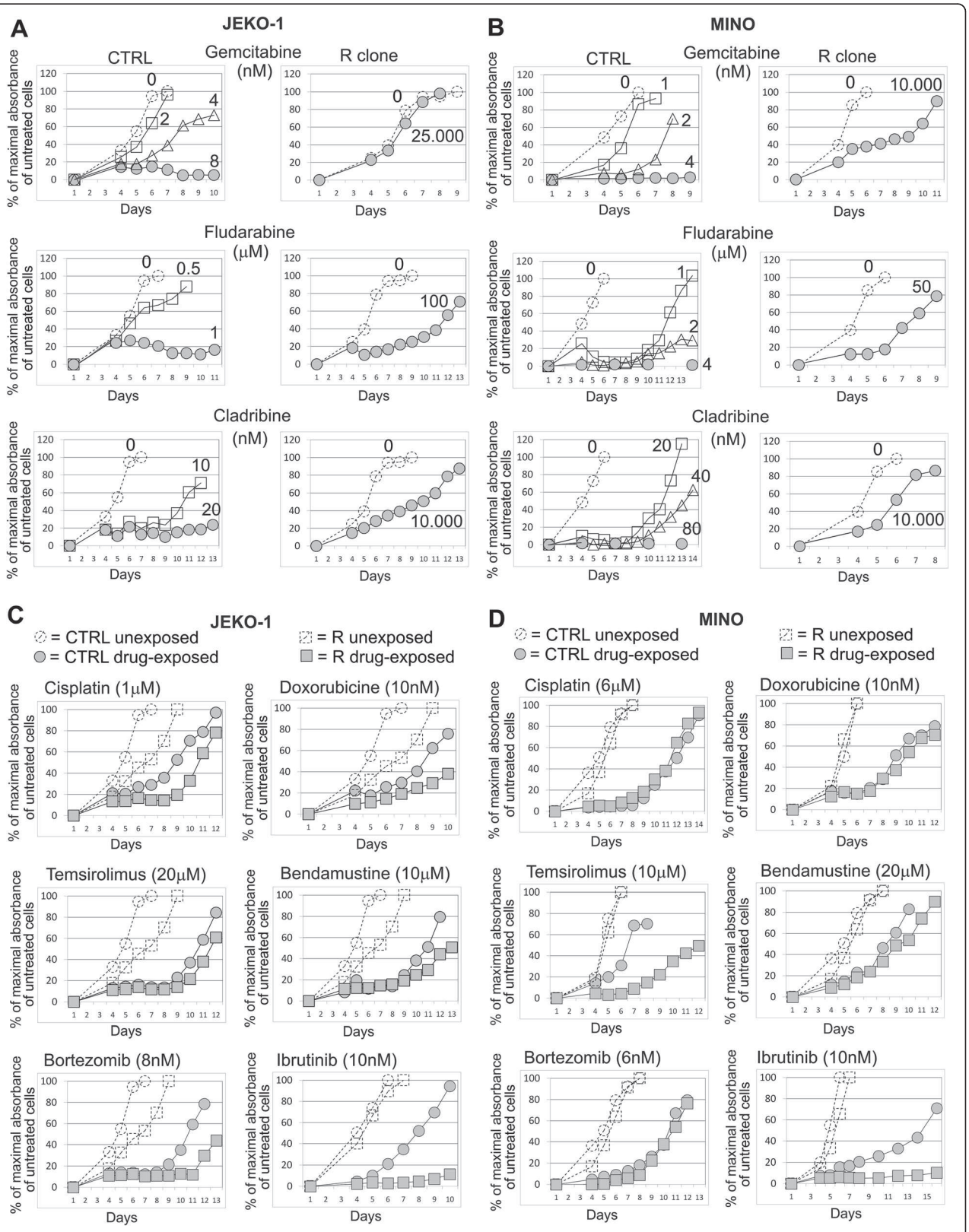

Figure 4 (See legend on next page.)

(See figure on previous page.)
Figure 4 R clones are cross-resistant to nucleoside analogs, but remain sensitive to other classes of anti-lymphoma agents. (A-D) WST-8 cell proliferation assays of CTRL cells and R clones were carried out as described in Methods. Maximal absorbance obtained from the untreated cells during the particular experiment (MAX_u) was arbitrary set as 100%. Absorbance of medium without cells was used as background **(B)**. For each cell population (both, unexposed and drug-exposed) and for each measurement (M_1, M_2, M_3…M_X) the proliferation curve was calculated as follows: (M_X - B)/(MAX_u - B). As a consequence, proliferation curves of untreated cells always peak at 100%, while proliferation curves of drug-exposed cells can terminate below or above 100%. One representative example of two independent experiments carried out both on JEKO-1 **(A, C)** and MINO **(B, D)** is shown. Data from the remaining three MCL cell lines (HBL-2, GRANTA-519 and REC-1) are not shown, because they did not significantly differ from those presented for the JEKO-1 and MINO cells. In summary, all 5 R clones were cross-resistant to the tested nucleoside analogs, but remained sensitive to other classes of anti-lymphoma agents with negligible differences between particular MCL cell lines. The only exception to the rule was markedly (>100-fold) increased sensitivity of REC-1 R clone to ibrutinib compared to REC-1 CTRL cells (see Additional file 3: Figure S2). The remaining 4 MCL cell lines (JEKO-1, MINO, GRANTA-519 and HBL-2) showed only approx. 2-fold increased sensitivity to ibrutinib compared to the corresponding CTRL cells. Standard deviations were < 5% for all measurements presented in Figure 4.

substrates of DCK explains the observed cross-resistance of R clones to all tested nucleoside analogs, both purine- and pyrimidine-derived. Retained sensitivity to other classes of anti-MCL agents (i.e. other than nucleoside analogs) with diverse molecular mechanisms of their respective antitumor activities suggests that no major additional molecular alteration was involved in the development of araC resistance.

Prognosis of patients with relapsed/refractory MCL (RR-MCL) is dismal. Currently there is no standard-of-care for RR-MCL patients. Second-line treatment approaches include fludarabine, gemcitabine, cladribine, cisplatin, bortezomib, temsirolimus, bendamustine, lenalidomide and ibrutinib-based regimen. We have proved *in vitro* and *in vivo* on a mouse xenograft model of MCL that treatment of patients, who progress on or relapse

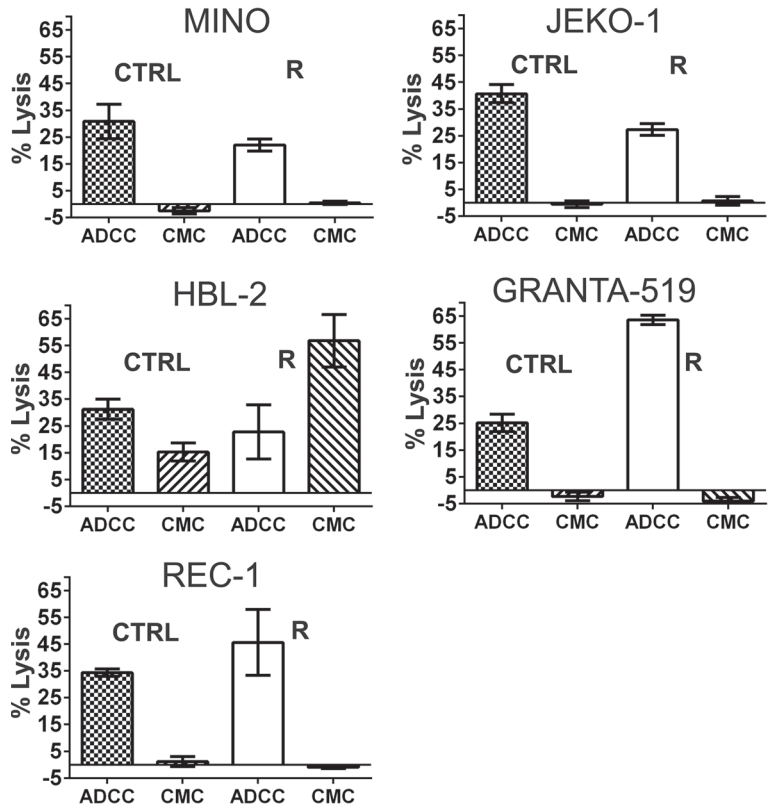

Figure 5 R clones remain sensitive to anti-CD20 monoclonal antibody rituximab. ^{51}Cr release assay was used to assess the impact of the anti-CD20 monoclonal antibody rituximab on complement mediated cytotoxicity (CMC) and antibody dependent cellular cytotoxicity (ADCC). CMC was measurable only in HBL-2 cells (both CTRL and R), but was negligible in the remaining four MCL cell populations (both CTRL and R). In HBL-2 R clone the CMC was significantly increased compared to CTRL. ADCC was measurable in all five MCL cell lines. In JEKO-1 R clone the ADCC was slightly decreased compared to CTRL. In GRANTA-519 R clone the ADCC was significantly increased compared to CTRL. In MINO, REC-1 and HBL-2 the ADCC remained comparable between R clone and CTRL cells.

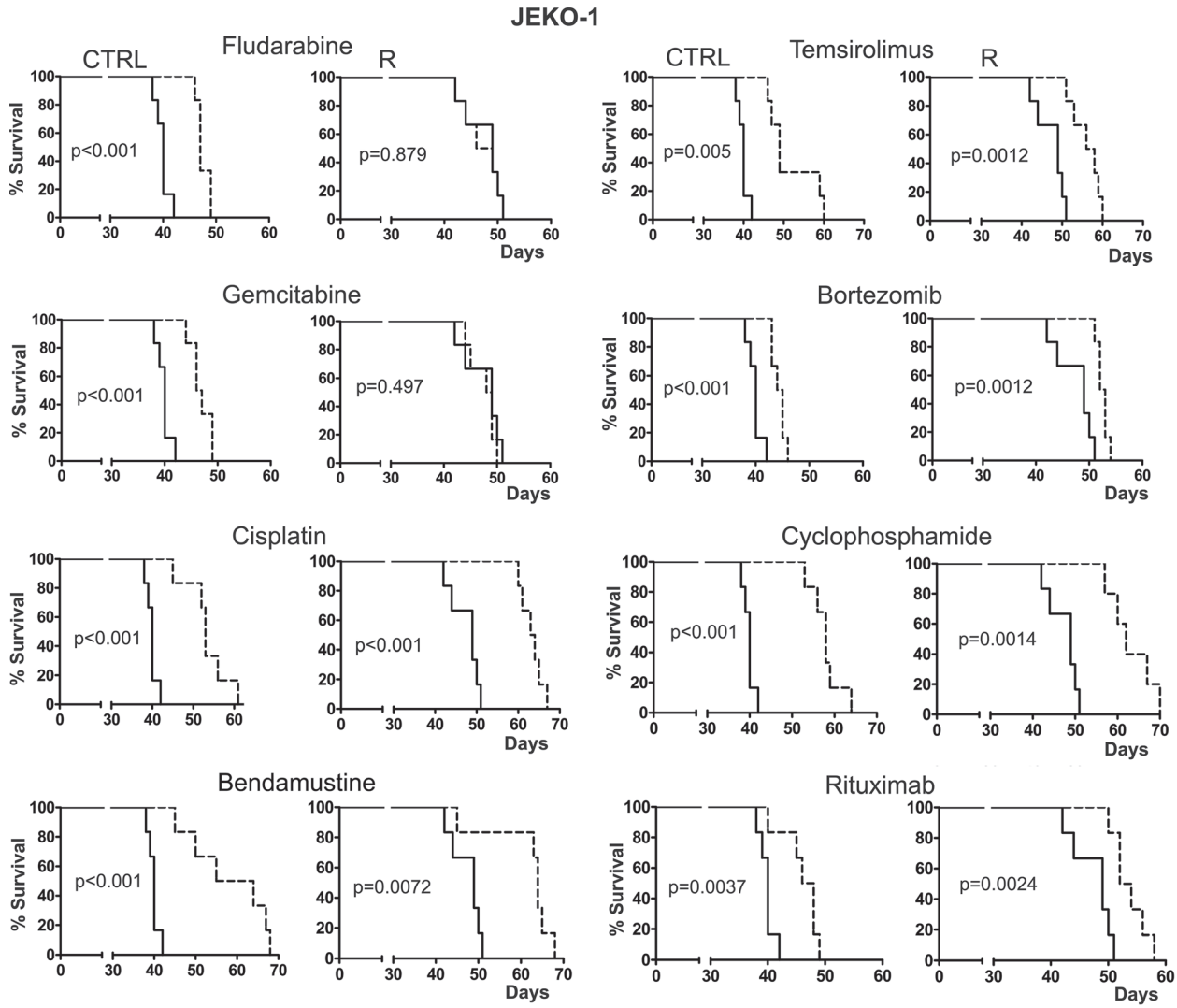

Figure 6 Experimental therapy of mice xenografted with JEKO-1 CTRL and JEKO-1 R cells. Overall survival of experimental animals is shown as Kaplan-Meier survival estimates. Loss of anti-tumor activity was observed for the nucleoside analogs fludarabine and gemcitabine in the therapy of R clone-xenografted mice (dashed lines) when compared to CTRL-xenografted mice (solid lines). Other classes of anti-lymphoma agents retained the antitumor activity in both CTRL- and R clone-xenografted mice. Individual cohorts contained 6 animals. For more details see Methods.

after high-dose araC-based regimen should not rely on nucleoside analogs, namely on the currently used agents fludarabine, gemcitabine and cladribine, since all of them must be phosphorylated by DCK to exert their anti-lymphoma activity. Instead, other classes of anti-lymphoma drugs should be applied in case of araC failure, i.e. in the setting of anticipated araC-resistance. Some of these agents have only recently been approved for the therapy of relapsed/refractory (RR-) MCL, temsirolimus in Europe, bortezomib and ibrutinib in USA. It might be speculated that high-dose therapy (given before autologous stem cell transplant) based on other agents than nucleoside analogs might prove more beneficial especially for those patients with suboptimal responses after induction araC-based immunochemotherapy (e.g. patients, who achieve partial remission, or patients with detectable minimal residual disease). In addition to the currently approved agents, bendamustine represents another extremely promising drug in MCL. Recently it was demonstrated that bendamustine potentiates the effect of araC by augmenting the level of intracellular ara-CTP, and the R-BAC (rituximab, bendamustine, araC) regimen was shown to be effective even in patients resistant to araC thus providing a treatment option even for the elderly and/or frail patients [16,30,31]. It might be speculated that the increased level of ara-CTP might partially offset the anticipated downregulation of DCK thereby explaining, why the combination of bendamustine and araC was shown to be effective even in patients, who relapsed after araC-based therapies [30].

Table 3 Gene expression analysis of DCK in a set of primary MCL samples obtained from patients before and after araC-based therapies

Sample at diagnosis	Source	ΔCT (DCK-GAPDH)	Therapy	Sample at relapse	Disease-free survival (months)	Source	ΔCT (DCK-GAPDH)	Difference in ΔCT between R and D samples
D1	PBMC	3.4	A*	R1	12	PBMC	3.7	+0.3
D2	PE***	3.3	A	R2	10	PE***	5.3	+2.0
D3	FFPE	0.1	A	R3	5	FFPE	1.3	+1.2
D4	FFPE	1.7	B	R4	4	FFPE	3.5	+1.8
D5	PBMC	1.4	A	R5	7	PBMC	2.2	+0.8
D6	PBMC	4.1	B**	R6	3	PBMC	3.9	−0.2
D7	FFPE	1.3	B	R7	13	FFPE	3.5	+2.2
D8	FFPE	2.0	A	R8	25	FFPE	1.8	−0.2
D9	PBMC	1.9	B	R9	N/A	PBMC	3.3	+1.4
D10	PBMC	2.3	A	R10	N/A	PBMC	1.5	−0.8

*A = alternation of R-CHOP and R-araC (2 g/m2, 2 doses a 24 h).
**B = Nordic protocol (alternation of R-MaxiCHOP and R-araC (2-3 g/m2, 4 doses a 12 h).
***PE pleural effusion (CD19-sorted).
Samples from relapsed patients were obtained at diagnosis (D1-D8) and at lymphoma relapse after failure of araC-based therapies (R1-R8). Samples from refractory patients were obtained from primary araC-resistant MCL patients before (D9-D10) and 14 days after (R9-R10) administration of high-dose araC. Real-time RT-PCR was used to determine changes in DCK expression.

Conclusions

Our data from the cell lines and primary MCL samples clearly demonstrate that acquired resistance of MCL cells to araC is associated with downregulation of mRNA and protein expression of DCK, enzyme of the nucleotide salvage pathway responsible for phosphorylation of most nucleoside analogs used in anti-cancer therapy. In translation, the results suggest that 1. nucleoside analogs should not be used for the second-line therapy of MCL patients, who fail after araC-based regimen; 2. non-nucleoside analogs should be employed in this setting, including cisplatin, ibrutinib, temsirolimus, bortezomib or bendamustine; 3. ibrutinib appears particularly effective in eliminating araC-resistant MCL cells.

Methods

Cell culture

JEKO-1, GRANTA-519 and REC-1 were purchased from German Collection of Microorganisms and Cell Cultures (DSMZ), MINO was from American Tissue Culture Collection (ATCC), HBL-2 was a kind gift of prof. Dreyling (University of Munich, Germany). Cell lines were cultured

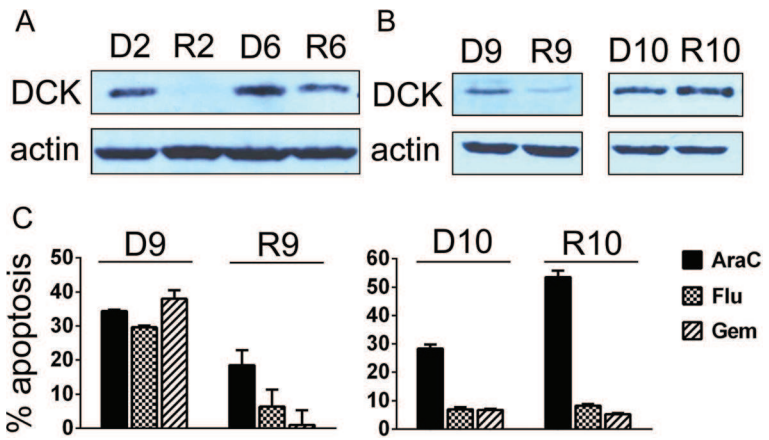

Figure 7 Protein expression of DCK in primary MCL samples, and their *ex vivo* sensitivity to nucleoside analogs. (A-B) Relative expression of deoxycytine kinase (DCK) in post-treatment primary MCL samples (R2, R6, R9, R10) compared to pre-treatment samples (D2, D6, D9, D10). **(C)** CD19-sorted PBMC cells were isolated from two leukemized araC-refractory MCL patients before (D9, D10) and 14 days after (R9, R10) administration of high-dose araC. The cells were *ex vivo/in vitro* exposed to araC (25 μM), fludarabine (Flu, 100 μM) and gemcitabine (Gem, 25 μM). Apoptosis was measured after 24 hours using standard Annexin-V-PE and flow cytometry. Apoptotic cells are shown as Annexin-V-PE-positive cells (Y axis). Basal apoptosis of drug-unexposed cells was subtracted from the apoptosis of the drug-exposed cells.

in Iscove's modified Dulbecco's medium (IMDM) supplemented with 15% fetal bovine serum (FBS) and 1% penicillin/streptomycin.

Reagents

Cytarabine, fludarabine, gemcitabine, cladribine, cyclophosphamide, doxorubicin and cisplatin were from Clinical Dept. of Hematology, University Hospital in Prague, Czech Republic. Temsirolimus, bortezomib, bendamustine and ibrutinib were purchased from Selleck Chemicals. Rituximab was kindly provided by Roche, Czech Republic.

Establishment of araC-resistant clones

MCL cell lines were incubated in Iscove's modified Dulbecco's medium (IMDM) supplemented with 15% fetal bovine serum with increasing concentrations of cytarabine up to 50 μM.

Proliferation assays

Proliferation was estimated using WST-8 Quick Cell Proliferation Assay Kit (BioVision) according to the manufacturer instructions. Briefly, 5.000 cells were seeded into 96-well plate on day 1. Drugs were added on day 1. Proliferation was measured on day 1 and then since day 4 daily. Antiproliferative activity of each drug was analyzed at several concentrations.

Absorbance of the triplicate samples was measured on ELISA reader after 3 hour incubation with WST-8 reagent at 37 grades Celsius in the thermostat. Maximal absorbance (MAX_u) obtained from the untreated cells during the particular experiment was arbitrary set as 100%. Absorbance of medium without cells was used as background (B). For each cell population (both, unexposed and drug-exposed) and for each measurement (M_1, M_2, M_3...M_X) the proliferation curve was calculated as follows: (M_X - B)/(MAX_u - B). As a consequence, the proliferation curve of untreated cells always peaks 100%, while proliferation curves of drug-exposed cells can terminate below or above 100%.

^{51}Cr release assay for the assessment of the impact that CD20 mAbs have on rituximab-mediated complement mediated cytotoxicity (CMC) and antibody dependent cellular cytotoxicity (ADCC)

CTRL MCL cells and R clones were labeled with ^{51}Cr at 37°C, 5% CO2 for 2 hrs. ^{51}Cr-labeled cells were then placed in 96-well plates at a cell concentration of 1×10^5 cells/well (complement-mediated cytotoxicity (CMC) assay) or 1×10^4 cells/well (antibody-dependent cell cytotoxicity (ADCC) assay). Cells were then exposed to rituximab (10 mg/ml) or isotype antibody (10 mg/ml) and human serum (for CMC assay, 1:4 dilution) or peripheral blood mononuclear cells (PBMCs) (for ADCC assay, 40:1 effector: target ratio) for six hrs at 37°C and 5% CO2. ^{51}Cr release was measured from the supernatant by standard gamma counting and the percentage of lysis was calculated. PBMCs were obtained from healthy donors (Roswell Park Cancer Institute IRB-approved protocol CIC-016) and isolated by Histopaque-1077 ultracentrifugation of peripheral whole blood and used at an effector: target ratio of 40:1 for ADCC assays. Pooled human serum was used as the source of complement for CMC assays.

Gene expression profiling and data analysis

A biological duplicate of each araC-resistant MCL clone (R) was compared to a biological duplicate of the original araC-sensitive (CTRL) cell line. In total, five R clones were compared to five corresponding CTRL cell lines using two microarray chips. Total RNA was extracted by RNeasy Mini Kit (Qiagen), and its quality verified using the Agilent 2100 Bioanalyzer (Agilent Technology). Extracted RNA was amplified using the Illumina RNA Amplification Kit (Ambion). Amplified RNA was hybridized to the Illumina HumanRef-8 and HumanRef-12 BeadChips (Illumina). Subsequent data analysis was performed in R-software, mainly in limma package from Bioconductor (http://www.bioconductor.org). Multiple testing correction was performed using Benjamini & Hochberg method. The filtered group of genes with fold change at least ±1.5-fold and adjusted p value < 0.05 were annotated and arranged into biologically relevant categories using The Database for Annotation, Visualization and Integrated Discovery (DAVID, http://david.abcc.ncifcrf.gov).

Primary MCL sample acquisition, real-time RT-PCR analysis, and apoptosis measurement

All primary MCL samples were obtained from patients with MCL at diagnosis (D1-D10), and at the relapse or during progression after failure of high-dose araC-based front-line therapies (R1-R10). Samples were obtained from patients, who signed informed consent according to the Declaration of Helsinki. Mononuclear cells were isolated from all PBMC and PE samples by the standard Ficoll-Hypaque gradient centrifugation. Mononuclear cells were then CD19 sorted on magnetic columns using CD19 microbeads (Miltenyi Biotec). The purity of MCL population after sorting was > 95% in all cases as verified by flow-cytometry. Total RNA was isolated from CD19-sorted PBMC or PE cells stored in RNA*later* solution using RNeasy Mini Kit (Qiagen, Hilden, Germany) and from fresh-frozen paraffin-embedded (FFPE) lymph node samples using High Pure RNA Paraffin Kit (Roche Diagnostics GmbH, Germany) according to the manufacturer's instructions. cDNA synthesis was carried out from 1 μg of total RNA with the High-Capacity cDNA Reverse Transcription Kit (random primers) (Applied Biosystems). Real-time RT-PCR was performed using TaqMan Gene Expression Assays on the ABI 7900HT detection system (Applied

Biosystems). The reference gene was GAPDH. *Ex vivo* apoptosis of primary MCL cells was determined using Annexin-V-PE (Apronex, Czech Republic) and flow cytometry (BD FACS Canto II) according to the manufacturer's instructions after 24 hours exposure to 25 μM araC, 100 μM fludarabine and 25 μM gemcitabine.

Experimental therapy of MCL xenografts

In vivo studies were approved by the institutional Animal Care and Use Committee. Immunodeficient NOD.Cg-*Prkdc*^{scid} *Il2rg*^{tm1Wjl}/SzJ mice (Jackson Laboratory) were maintained in individually ventilated cages. JEKO-1 cell line-based mouse model of MCL was used for experiments [32]. JEKO-1 cells were harvested, suspended in PBS, and injected (1×10^6/mouse) i.v. into tail vein of 8- to 12-week-old female mice on DAY 1. Therapy was initiated on DAY 8. Each cohort of mice contained 6–8 animals. The mice received treatment as follows: temsirolimus 1 mg s.c. 1 x weekly (3 cycles), cyclophosphamide 3 mg i.p. 1 × weekly (3 cycles), bendamustine 0.5 mg i.p. two subsequent days (day 1 + day 2) every two weeks (2 cycles), bortezomib 25 μg i.p. 2 × weekly (3 cycles), cisplatin 180 μg i.p. every two weeks (2 cycles), gemcitabine 10 mg i.p. 1 × weekly (3 cycles), fludarabine 1 mg three subsequent days (day 1–3) weekly (3 cycles), rituximab 250 μg s.c. 1 × weekly (3 cycles). The data were analysed in GraphPad Software.

Two-dimensional electrophoresis

IPG strips (pH 4.0-7.0, 24 cm; ReadyStrip, Bio-Rad) were rehydrated overnight in 450 μL of sample, representing 1.5 mg of protein. Isoelectric focusing was performed for 70 kVh using Protean IEF cell (Bio-Rad). Six replicates were run for each cell type. Focused strips were equilibrated and reduced in equilibration (6 M urea, 50 mM Tris pH 8.8, 30% glycerol, 2% SDS) supplemented with DTT (450 mg per 50 mL) for 15 min and then alkyled in equilibration buffer with added iodacetamide (1.125 mg iodacetamide per 50 mL). SDS-PAGE electrophoresis was performed in a Tris-glycine-SDS system using a 12-gel Protean Dodeca Cell apparatus (Bio-Rad) with buffer circulation and external cooling (20°C). Gels were run at a constant voltage of 80 V per gel for 30 min and then at a constant voltage of 200 V for 6 h. Gels were washed in deionized water to remove redundant SDS and with colloidal Coomassie Brilliant Blue (SimplyBlue™ Safestain, Invitrogen, Carlsbad, CA, USA) overnight.

Gel image analysis and extraction of peptides

Stained gels were scanned with GS 800 calibrated densitometer (Bio-Rad) and image analysis was performed with Progenesis™ software (Nonlinear Dynamics, Ltd., Newcastle upon Tyne, UK) in semi-manual mode with 6 gel replicates for each cell type. Normalization of gel images was based on total spot density, and integrated spot density values (spot volumes) were then calculated after background subtraction. Average spot volume values (averages from the all 6 gels in the group) for each spot were compared between the groups. Protein spots were considered differentially expressed if their average normalized spot volume difference was > 2-fold. As determined by the Student's t-test, a p-value < 0.05 was considered to indicate a statistically significant difference.

Protein digestion and peptide extraction

Spots containing differentially expressed proteins were excised from the gels, cut into small pieces and washed 3 times with 25 mM ammonium bicarbonate in 50% acetonitrile (ACN). The gels were then dried in a Speed-Vac Concentrator (Eppendorf, Hamburg, Germany). Sequencing grade modified trypsin (Promega, Madison, WI, USA) (6 ng/μl in 25 mM ammonium bicarbonate in 5% ACN) was added. Following overnight incubation at 37°C, the resulting peptides were extracted with 50% ACN.

MS analysis and protein identification

Peptide samples were spotted on a steel target plate (Bruker Daltonics, Bremen, Germany) and allowed to dry at room temperature. Matrix solution (3 mg α-cyano-4-hydroxycinnamic acid in 1 ml of 50% ACN containing 0.1% trifluoroacetic acid) was then added. MS was performed on an Autoflex II MALDI-TOF/TOF mass spectrometer (Bruker Daltonics, Bremen, Germany) using a solid nitrogen laser (337 nm) and FlexControl software in reflectron mode with positive ion mass spectra detection. The mass spectrometer was externally calibrated with Peptide Calibration Standard II (Bruker Daltonics). Spectra were acquired in the mass range 800–3,000 Da. The peak lists were generated using FlexAnalysis and searched against Swiss-Prot (2012_07 version, 536 789 sequences) using Mascot software. The peptide mass tolerance was set to 100 ppm, taxonomy Homo sapiens, missed cleavage was set to 1, fixed modification for cysteine carbamidomethylation, and variable modifications for methionine oxidation and protein N-terminal acetylation. Proteins with Mascot score over the threshold 56 for $p < 0.05$ calculated for the used settings were considered as identified. If the score was lower, the identity of protein candidate was confirmed by MS/MS.

Western blot analysis

Cells were lysed in NHT buffer (140 mM NaCl, 10 mM HEPES, 1.5% Triton X-100, pH 7.4). Protein concentration in the collected supernatants was determined by the Bradford assay (Bio-Rad). Lysate samples (50 μg) were combined with SDS loading buffer containing 2-mercaptoethanol and boiled for 5 min. Quadruplicate samples were separated on 12% SDS-PAGE minigels in Tris-glycine buffer (Bio-Rad).

Electrophoresis was performed at a constant voltage for 30 min at 45 V per gel, and then at 90 V per gel until the dye front reached the gel bottom. Proteins were transferred onto 0.45 μm PVDF membranes (Milipore, Billerica, MA, USA) in a semi-dry blotter (Hoefer, San Francisco, CA, USA) at 0.8 mA/cm^2. Membranes were incubated in PBS (Invitrogen) containing 0.1% Tween-20 and 5% non-fat dried milk for 1 h. GAPDH or Actin were used as the loading controls. As primary antibodies anti-deoxycytidine kinase mouse monoclonal antibody (sc 81245 Santa Cruz Biotechnology, Sanat Cruz, CA, USA) diluted 1:200 or polyclonal anti-GAPDH produced in rabbit (Sigma-Aldrich, G9545) diluted 1:10,000 were used. After thorough washing in blocking buffer, a secondary horseradish peroxidase-conjugated anti-mouse (sc2005) or anti-rabbit antibody (sc2313) (both from Santa Cruz Biotechnology) was added (1:10,000). The signal was detected using LumiGLO Reserve, (KPL, Gaithersburg, MD, USA) or Western Blotting Luminol Reagent (Santa Cruz Biotechnology, Inc., Santa Cruz, CA, USA) and membranes were exposed to X-ray films (Kodak, Rochester, NY, USA).

Additional files

Additional file 1: Figure S1. Functional cathegories of genes differentially expressed in R compared to CTRL as determined by DAVID. The filtered group of genes acquired from all five MCL cell lines with fold change at least ±1.5-fold and adjusted p value < 0.05 were annotated and arranged into biologically relevant categories using The Database for Annotation, Visualization and Integrated Discovery (DAVID, http://david.abcc.ncifcrf.gov).

Additional file 2: Table S1. List of genes differentially expressed in more than one R clone compared to the corresponding CTRL cells. Microarray data are shown in Additional file 2: Table S1. 31 genes were differentially expressed in two araC-resistant clones (R) compared to the corresponding araC-sensitive controls (CTRL). 1 gene (TPM1) was differentially expressed in three R clones, and 1 gene (DCK) was differentially expressed in all five R clones compared to the corresponding CTRL.

Additional file 3: Figure S2. Ibrutinib appears more cytotoxic to cytarabine-resistant (R) compared to cytarabine-sensitive (CTRL) MCL cells. WST-8 cell proliferation assays of CTRL cells and R clones were carried out as described in Methods. Maximal absorbance obtained from the untreated cells during the particular experiment (MAX_u) was arbitrary set as 100%. Absorbance of medium without cells was used as background (B). For each cell population (both, unexposed and drug-exposed) and for each measurement (M_1, M_2, M_3…M_X) the proliferation curve was calculated as follows: (M_X - B)/(MAX_u - B). As a consequence, proliferation curves of untreated cells always peak at 100%, while proliferation curves of drug-exposed cells can terminate below or above 100%. One representative example of two independent experiments carried out on REC-1, HBL-2 and GRANTA-519 is shown. In summary, REC-1 R clone was > 100-fold sensitive to Bruton tyrosine-kinase (BTK) inhibitor ibrutinib compared to REC-1 CTRL cells. Both HBL-2 and GRANTA-519 R clones were approx. 2-fold more sensitive to ibrutinib compared to HBL-2 and GRANTA-519 CTRL cells.

Abbreviations

ACN: Acetonitrile; ADCC: Antibody-dependent cytotoxicity; AML: Acute myelogeneous leukemia; BTK: Bruton tyrosine-kinase; araC: Cytarabine, a pyrimidine analog used for anticancer therapy; CDA: Cytidine-deaminase, a key inactivating enzyme of nucleotide salvage pathway; CMC: Complement-mediated cototoxicity; CTRL: araC-sensitive MCL cell line; DCK: Deoxycytidine-kinase, a rate-limiting enzyme of nucleotide salvage pathway; DTT: Dithiothreitol; FFPE: Fresh-frozen paraffin-embedded (lymph node sections); HDAC: High-dose araC; i.v.: Intravenous injection; MCL: Mantle cell lymphoma; NHL: Non-Hodgkin lymphoma; NT5C2: Cytoplasmic 5′nucleotidase II, a key inactivating enzyme of nucleotide salvage pathway; PBMC: Peripheral-blood mononuclear cells; PE: Pleural effusion; R: araC-resistant clone derived from araC-sensitive cell line; R-CHOP: A combination of rituximab, cyclophosphamide, doxorubicin, vincristin and prednisone; R-DHAP: A combination of rituximab, high-dose cytarabine, cisplatin and dexamethasone; RR-MCL: Relapsed/refractory mantle cell lymphoma; s.c.: subcutanous injection.

Competing interests

The authors declare that they have no competing interests.

Authors' contributions

PK and JP conceived of the study and participated in drafting of the manuscript. MK carried out gene expression analysis and *in vivo* experiments, OV, LL and JP carried out proteomic analysis and western blotting. BM, DV, JM, PV and LL participated in *in vitro* experiments. CM carried out chrome-releasing assays. VK performed the statistical analysis. FH and MV participated in the design of the study and helped to review the manuscript. RJ and MT carried out analysis of primary MCL samples. All authors read and approved the final manuscript.

Authors' informations

Jiri Petrak and Pavel Klener Jr are considered senior co-authors.

Acknowledgements

Financial Support: IGA-MZ NT13201-4/2012, GACR14-19590S, GA-UK 446211, GA-UK 253284 700712, GA-UK 595912, GA-UK 1270214, UNCE 204021, PRVOUK-27/LF1/1, PRVOUK P24/LF1/3, SVV-2013-266509 and BIOCEV – Biotechnology and Biomedicine Centre of the Academy of Sciences and Charles University in Vestec" (CZ.1.05/1.1.00/02.0109), from the European Regional Development Fund.

Author details

[1]Institute of Pathological Physiology, Charles University in Prague, First Faculty of Medicine, Prague, Czech Republic. [2]First Department of Medicine - Department of Hematology, General University Hospital and Charles University in Prague, Prague, Czech Republic. [3]Institute of Pathology, General University Hospital and Charles University in Prague, Prague, Czech Republic. [4]Departments of Immunology and Medicine, Roswell Park Cancer Institute, Buffalo, NY, USA. [5]Institute of Hematology and Blood Transfusion, Prague, Czech Republic.

Received: 29 January 2014 Accepted: 23 June 2014
Published: 27 June 2014

References

1. Dreyling M, Kluin-Nelemans HC, Beà S, Klapper W, Vogt N, Delfau-Larue M-H, Hutter G, Cheah C, Chiappella A, Cortelazzo S, Pott C, Hess G, Visco C, Vitolo U, Klener P, Aurer I, Unterhalt M, Ribrag V, Hoster E, Hermine O: **Update on the molecular pathogenesis and clinical treatment of mantle cell lymphoma: report of the 11th annual conference of the European Mantle Cell Lymphoma Network.** *Leuk Lymphoma* 2013, **54:**699–707.
2. Jares P, Colomer D, Campo E: **Molecular pathogenesis of mantle cell lymphoma.** *J Clin Invest* 2012, **122:**3416–3423.
3. Delarue R, Haioun C, Ribrag V, Brice P, Delmer A, Tilly H, Salles G, Van Hoof A, Casasnovas O, Brousse N, Lefrere F, Hermine O: **CHOP and DHAP plus rituximab followed by autologous stem cell transplantation in mantle cell lymphoma: a phase 2 study from the Groupe d'Etude des Lymphomes de l'Adulte.** *Blood* 2013, **121:**48–53.
4. Lefrère F, Delmer A, Suzan F, Levy V, Belanger C, Djabarri M, Arnulf B, Damaj G, Maillard N, Ribrag V, Janvier M, Sebban C, Casasnovas R-O, Bouabdallah R, Dreyfus F, Verkarre V, Delabesse E, Valensi F, McIntyre E, Brousse N, Varet B, Hermine O: **Sequential chemotherapy by CHOP and DHAP regimens followed by high-dose therapy with stem cell transplantation induces a high rate of complete response and improves event-free survival in mantle cell lymphoma: a prospective study.** *Leukemia* 2002, **16:**587–593.
5. Merli F, Luminari S, Ilariucci F, Petrini M, Visco C, Ambrosetti A, Stelitano C, Caracciolo F, Di Renzo N, Angrilli F, Carella AM, Capodanno I, Barbolini E,

Galimberti S, Federico M: **Rituximab plus HyperCVAD alternating with high dose cytarabine and methotrexate for the initial treatment of patients with mantle cell lymphoma, a multicentre trial from Gruppo Italiano Studio Linfomi.** *Br J Haematol* 2012, **156:**346–353.
6. Ferrero S, Dreyling M: **The current therapeutic scenario for relapsed mantle cell lymphoma.** *Curr Opin Oncol* 2013, **25:**452–462.
7. Wang ML, Rule S, Martin P, Goy A, Auer R, Kahl BS, Jurczak W, Advani RH, Romaguera JE, Williams ME, Barrientos JC, Chmielowska E, Radford J, Stilgenbauer S, Dreyling M, Jedrzejczak WW, Johnson P, Spurgeon SE, Li L, Zhang L, Newberry K, Ou Z, Cheng N, Fang B, McGreivy J, Clow F, Buggy JJ, Chang BY, Beaupre DM, Kunkel LA, Blum KA: **Targeting BTK with ibrutinib in relapsed or refractory mantle-cell lymphoma.** *N Engl J Med* 2013, **369:**507–516.
8. Goy A, Sinha R, Williams ME, Kalayoglu Besisik S, Drach J, Ramchandren R, Zhang L, Cicero S, Fu T, Witzig TE: **Single-agent lenalidomide in patients with mantle-cell lymphoma who relapsed or progressed after or were refractory to Bortezomib: phase II MCL-001 (EMERGE) study.** *J Clin Oncol* 2013, **31:**3688–3695.
9. Goy A, Younes A, McLaughlin P, Pro B, Romaguera JE, Hagemeister F, Fayad L, Dang NH, Samaniego F, Wang M, Broglio K, Samuels B, Gilles F, Sarris AH, Hart S, Trehu E, Schenkein D, Cabanillas F, Rodriguez AM: **Phase II study of proteasome inhibitor bortezomib in relapsed or refractory B-cell non-Hodgkin's lymphoma.** *J Clin Oncol* 2005, **23:**667–675.
10. Ansell SM, Tang H, Kurtin PJ, Koenig PA, Inwards DJ, Shah K, Ziesmer SC, Feldman AL, Rao R, Gupta M, Erlichman C, Witzig TE: **Temsirolimus and rituximab in patients with relapsed or refractory mantle cell lymphoma: a phase 2 study.** *Lancet Oncol* 2011, **12:**361–368.
11. Witzig TE, Geyer SM, Ghobrial I, Inwards DJ, Fonseca R, Kurtin P, Ansell SM, Luyun R, Flynn PJ, Morton RF, Dakhil SR, Gross H, Kaufmann SH: **Phase II trial of single-agent temsirolimus (CCI-779) for relapsed mantle cell lymphoma.** *J Clin Oncol* 2005, **23:**5347–5356.
12. Vose JM: **Mantle cell lymphoma: 2012 update on diagnosis, risk-stratification, and clinical management.** *Am J Hematol* 2012, **87:**604–609.
13. Robak T, Lech-Maranda E, Janus A, Blonski J, Wierzbowska A, Gora-Tybor J: **Cladribine combined with cyclophosphamide and mitoxantrone is an active salvage therapy in advanced non-Hodgkin's lymphoma.** *Leuk Lymphoma* 2007, **48:**1092–1101.
14. Morschhauser F, Depil S, Jourdan E, Wetterwald M, Bouabdallah R, Marit G, Solal-Céligny P, Sebban C, Coiffier B, Chouaki N, Bauters F, Dumontet C: **Phase II study of gemcitabine-dexamethasone with or without cisplatin in relapsed or refractory mantle cell lymphoma.** *Ann Oncol* 2007, **18:**370–375.
15. Johnson SA: **Use of fludarabine in the treatment of mantle cell lymphoma, Waldenström's macroglobulinemia and other uncommon B- and T-cell lymphoid malignancies.** *Hematol J* 2004, **5**(Suppl 1):S50–S61.
16. Visco C, Finotto S, Zambello R, Paolini R, Menin A, Zanotti R, Zaja F, Semenzato G, Pizzolo G, D'Amore ESG, Rodeghiero F: **Combination of rituximab, bendamustine, and cytarabine for patients with mantle-cell non-Hodgkin lymphoma ineligible for intensive regimens or autologous transplantation.** *J Clin Oncol* 2013, **31:**1442–1449.
17. Ellison RR, Holland JF, Weil M, Jacquillat C, Boiron M, Bernard J, Sawitsky A, Rosner F, Gussoff B, Silver RT, Karanas A, Cuttner J, Spurr CL, Hayes DM, Blom J, Leone LA, Haurani F, Kyle R, Hutchison JL, Forcier RJ, Moon JH: **Arabinosyl cytosine: a useful agent in the treatment of acute leukemia in adults.** *Blood* 1968, **32:**507–523.
18. Kantarjian H, Barlogie B, Plunkett W, Velasquez W, McLaughlin P, Riggs S, Cabanillas F: **High-dose cytosine arabinoside in non-Hodgkin's lymphoma.** *J Clin Oncol* 1983, **1:**689–694.
19. Capizzi RL: **Curative chemotherapy for acute myeloid leukemia: the development of high-dose ara-C from the laboratory to bedside.** *Invest New Drugs* 1996, **14:**249–256.
20. Lamba JK: **Genetic factors influencing cytarabine therapy.** *Pharmacogenomics* 2009, **10:**1657–1674.
21. Clarke ML, Damaraju VL, Zhang J, Mowles D, Tackaberry T, Lang T, Smith KM, Young JD, Tomkinson B, Cass CE: **The role of human nucleoside transporters in cellular uptake of 4′-thio-beta-D-arabinofuranosylcytosine and beta-D-arabinosylcytosine.** *Mol Pharmacol* 2006, **70:**303–310.
22. Capizzi RL, White JC, Powell BL, Perrino F: **Effect of dose on the pharmacokinetic and pharmacodynamic effects of cytarabine.** *Semin Hematol* 1991, **28**(3 Suppl 4):54–69.
23. Cai J, Damaraju VL, Groulx N, Mowles D, Peng Y, Robins MJ, Cass CE, Gros P: **Two distinct molecular mechanisms underlying cytarabine resistance in human leukemic cells.** *Cancer Res* 2008, **68:**2349–2357.
24. Hubeek I, Stam RW, Peters GJ, Broekhuizen R, Meijerink JPP, van Wering ER, Gibson BES, Creutzig U, Zwaan CM, Cloos J, Kuik DJ, Pieters R, Kaspers GJL: **The human equilibrative nucleoside transporter 1 mediates in vitro cytarabine sensitivity in childhood acute myeloid leukaemia.** *Br J Cancer* 2005, **93:**1388–1394.
25. Tang J, Xie X, Zhang X, Qiao X, Jiang S, Shi W, Shao Y, Zhou X: **Long term cultured HL-60 cells are intrinsically resistant to Ara-C through high CDA activity.** *Front Biosci (Landmark Ed)* 2012, **17:**569–574.
26. DeAngelis LM, Kreis W, Chan K, Dantis E, Akerman S: **Pharmacokinetics of ara-C and ara-U in plasma and CSF after high-dose administration of cytosine arabinoside.** *Cancer Chemother Pharmacol* 1992, **29:**173–177.
27. Qin T, Jelinek J, Si J, Shu J, Issa JP: **Mechanisms of resistance to 5-aza-2′-deoxycytidine in human cancer cell lines.** *Blood* 2009, **113**(3):659–667.
28. Ewald B, Sampath D, Plunkett W: **Nucleoside analogs: molecular mechanisms signaling cell death.** *Oncogene* 2008, **27:**6522–6537.
29. Galmarini CM, Mackey JR, Dumontet C: **Nucleoside analogues: mechanisms of drug resistance and reversal strategies.** *Leukemia* 2001, **15:**875–890.
30. Visco C, Castegnaro S, Chieregato K, Bernardi M, Albiero E, Zanon C, Madeo D, Rodeghiero F: **The cytotoxic effects of bendamustine in combination with cytarabine in mantle cell lymphoma cell lines.** *Blood Cells Mol Dis* 2012, **48:**68–75.
31. Hiraoka N, Kikuchi J, Yamauchi T, Koyama D, Wada T, Uesawa M, Akutsu M, Mori S, Nakamura Y, Ueda T, Kano Y, Furukawa Y: **Purine analog-like properties of bendamustine underlie rapid activation of DNA damage response and synergistic effects with pyrimidine analogues in lymphoid malignancies.** *PLoS One* 2014, **9:**1–14.
32. Klanova M, Soukup T, Jaksa R, Molinsky J, Lateckova L, Maswabi BC, Prukova D, Brezinova J, Michalova K, Vockova P, Hernandez-Ilizaliturri F, Kulvait V, Zivny J, Vokurka M, Necas E, Trneny M, Klener P: **Mouse models of mantle cell lymphoma, complex changes in gene expression and phenotype of engrafted MCL cells: implications for preclinical research.** *Lab Invest* in press.

doi:10.1186/1476-4598-13-159
Cite this article as: Klanova *et al.*: Downregulation of deoxycytidine kinase in cytarabine-resistant mantle cell lymphoma cells confers cross-resistance to nucleoside analogs gemcitabine, fludarabine and cladribine, but not to other classes of anti-lymphoma agents. *Molecular Cancer* 2014 **13**:159.

Resistance to TRAIL in mantle cell lymphoma cells is associated with the decreased expression of purine metabolism enzymes

JANA POSPISILOVA[1], ONDREJ VIT[1], LUCIE LORKOVA[1], MAGDALENA KLANOVA[1], JAN ZIVNY[1], PAVEL KLENER[1] and JIRI PETRAK[1,2]

[1]Institute of Pathological Physiology, First Faculty of Medicine, Charles University in Prague, 128 53 Prague; [2]Institute of Hematology and Blood Transfusion, 128 20 Prague, Czech Republic

Received January 25, 2013; Accepted March 1, 2013

DOI: 10.3892/ijmm.2013.1302

Abstract. Mantle cell lymphoma (MCL) is a rare aggressive type of B-cell non-Hodgkin's lymphoma. Response to chemotherapy tends to be short and virtually all patients sooner or later relapse. The prognosis of relapsed patients is extremely poor. The tumor necrosis factor-related apoptosis-inducing ligand (TRAIL) is considered one of the novel experimental molecules with strong antitumor effects. TRAIL triggers extrinsic apoptotis in tumor cells by binding to TRAIL 'death receptors' on the cell surface. Recombinant TRAIL has shown promising pro-apoptotic effects in a variety of malignancies including lymphoma. However, as with other drugs, lymphoma cells can develop resistance to TRAIL. Therefore, the aim of this study was to identify the molecular mechanisms responsible for, and associated with TRAIL resistance in MCL cells. If identified, these features may be used as molecular targets for the effective elimination of TRAIL-resistant lymphoma cells. From an established TRAIL-sensitive mantle cell lymphoma cell line (HBL-2) we derived a TRAIL-resistant HBL-2/R subclone. By TRAIL receptor analysis and differential proteomic analysis of HBL-2 and HBL-2/R cells we revealed a marked downregulation of all TRAIL receptors and, among others, the decreased expression of 3 key enzymes of purine nucleotide metabolism, namely purine nucleoside phosphorylase, adenine phosphoribosyltransferase and inosine-5'-monophosphate dehydrogenase 2, in the resistant HBL-2/R cells. The downregulation of the 3 key enzymes of purine metabolism can have profound effects on nucleotide homeostasis in TRAIL-resistant lymphoma cells and can render such cells vulnerable to any further disruption of purine nucleotide metabolism. This pathway represents a 'weakness' of the TRAIL-resistant MCL cells and has potential as a therapeutic target for the selective elimination of such cells.

Correspondence to: Ms. Jana Pospisilova, Institute of Pathological Physiology, First Faculty of Medicine, Charles University in Prague, U Nemocnice 5, 128 53 Prague, Czech Republic
E-mail: jana.pospisilova@lf1.cuni.cz

Key words: mantle cell lymphoma, TRAIL, drug resistance, purine nucleotide metabolism, proteomics

Introduction

Mantle cell lymphoma (MCL) is a rare agressive type of B-cell non-Hodgkin's lymphoma with an estimated annual incidence in Europe of 0.45/100,000 individuals (1). MCL is a biologically and clinically heterogeneous disease; the immunophenotype of neoplastic cells reflects the phenotype of cells similar to lymphocytes in the mantle zone of normal germinal follicles (2). The genetic hallmark of MCL cells is a translocation between chromosomes 11 and 14, t(11;14)(q13;q32), juxtaposing the gene for immunoglobulin heavy chain and the gene encoding cyclin D1. This results in cyclin D1 overexpression (3,4).

The standard of care for newly diagnosed MCL patients is combined immunochemotherapy alternating rituximab-CHOP (R-CHOP; cyclophosphamide, vincristine, doxorubicin and prednisone) and R-HDAC (high-dose cytarabine). The addition of rituximab and HDAC to CHOP has improved the survival of MCL patients in the last 2 decades from 3 to 5 years. However, the response to therapy tends to be short and virtually all patients sooner or later relapse. There is no standard of care for relapsed or refractory MCL patients. Salvage therapy usually comprises diverse regimens based on fludarabine, gemcitabine, cisplatin, bendamustine, bortezomib (inhibitor of 26S proteasome) or temsirolimus (inhibitor of mTOR). Recently, several new experimental molecules have shown promise in the therapy of relapsed or resistant MCL, including lenalidomide (immunomodulatory agent), ibrutinib (PCI-32765, inhibitor of Bruton's tyrosine-kinase), new monoclonal antibodies (e.g., anti-CD20 ofatumumab), as well as other agents (5). Combination therapies are currently being evaluated in clinical trials; however, novel drugs are required.

The tumor necrosis factor-related apoptosis-inducing ligand (TRAIL) is considered one of the novel experimental molecules with strong antitumor effects. TRAIL is a type II transmembrane protein from the tumor necrosis factor superfamily (6,7) expressed mostly by cells of the immune system (natural killer cells, cytotoxic T-cells, macrophages and dendritic cells). The main function of this molecule is thought to be in tumor immunosurveillance, but its actual molecular role remains to be elucidated.

TRAIL can trigger extrinsic apoptotis in target cells by binding to TRAIL death receptors located on the cell surface (8). This interaction is performed by a long extracellular C-terminal

region of the TRAIL molecule. There are 4 distinct cell surface TRAIL receptors in humans (DcR1, DcR2, DR4 and DR5) encoded by separate genes (9,10). However, only DR4 and DR5 contain a functional death domain (structurally conserved protein interaction domain) and are capable of signaling apoptosis. Two decoy receptors (DcR1 and DcR2) lack a functional death domain and inhibit TRAIL signaling by competing with death receptors for TRAIL (9,10). The binding of TRAIL to DR4 or DR5 leads to receptor homotrimerization and formation of the death-inducing signaling complex (DISC) (11). Through the DISC a caspase machinery is activated, which results in apoptosis (12). TRAIL death receptors DR4 and DR5 are ubiquitously expressed, indicating that most tissues and cell types are potential targets of TRAIL signaling (13). Nevertheless, TRAIL seems to induce apoptosis only in tumor cells but not in healthy tissues. Due to its selective pro-apoptotic effect, TRAIL has attracted much attention for its possible use in cancer therapy. *In vitro*, a recombinant soluble TRAIL molecule has shown cytostatic or cytotoxic effects in a wide variety of tumor cell lines, including leukemia and lymphoma cells, but not in normal cells (6,7,10,11,14-19). The administration of a recombinant soluble TRAIL molecule has been shown to induce the regression or complete remission of tumors in tumor xenograft models (11,20-26). The efficacy of recombinant TRAIL and agonistic antibodies recognizing either receptor DR4 or DR5 has been investigated in numerous clinical trials, as recently reviewed (27).

TRAIL has also shown promising pro-apoptotic effects in a variety of lymphoma cell lines including MCL (15). However, as with other drugs, cancer cells can develop resistance to TRAIL following prolonged exposure to sublethal doses of TRAIL (14,28). Resistance to TRAIL-mediated apoptosis can arise due to changes at the cell membrane level (typically by loss of expression or mutation of functional DR4 and/or DR5 at the cell surface) or on the intracellular level (such as incorrect formation of DISC and abberant expression of caspases) (29). The successful therapy of malignancies in general, and particularly those with very poor prognosis, such as MCL, depends on the effective management of drug resistance. An in-depth understanding of the processes involved in the development of drug resistance and a detailed description of secondary molecular changes associated with resistance are essential for successful cancer therapy. Specific molecular changes which occur in drug-resistant cells can confer a potential selective disadvatage to such cells and may be used as targets for the effective elimination of drug-resistant lymphoma cells.

The aim of this study was to elucidate the molecular mechanisms responsible for TRAIL resistance in MCL cells, as well as the secondary molecular alterations associated with this process. We also aimed to identify the phenotypic features specific for TRAIL-resistant MCL cells. If identified, these molecular features can be, at least theoretically, used as molecular targets for the effective elimination of TRAIL-resistant lymphoma cells in experimental therapies.

Materials and methods

Cell growth and cellular toxicity assay. HBL-2 cells were grown in Iscove's modified Dulbecco's medium in the presence of 10% foetal bovine serum, 1% penicillin-streptomycin solution in a 37˚C humidified atmosphere with 5% CO_2. TRAIL-resistant HBL-2/R cells were derived by selective pressure of increasing concentrations of human recombinant TRAIL (Apronex Biotechnologies, Czech Republic) up to 1,000 ng/ml in medium from the wild-type HBL-2 cells in 5 weeks. The toxicity of TRAIL to HBL-2 and HBL-2/R was measured using the colorimetric WST-8-based Quick Cell proliferation Assay kit II (BioVision, San Francisco, CA, USA) according to the manufacturer's instructions. Briefly, 40,000 cells were seeded in a 96-well plate in 300 μl of medium supplemented with increased concentrations of TRAIL up to 1,000 ng/ml in medium for 1-4 days. After the addition of WST reagent, absorbance was measured on a Sunrise microplate absorbance reader (Tecan Group Ltd., Männedorf, Switzerland) with a 450 nm reading filter and 630 nm reference filter. The absorbance of free medium was used as the background level, triplicate samples were grown and measured for each cell type and TRAIL concentration. Mean values were calculated. All chemicals were purchased from Sigma-Aldrich (St. Louis, MO, USA) unless specified otherwise.

Flow cytometric analysis. HBL-2 and HBL-2/R cells ($2x10^5$ cells for each assay) were washed in PBS buffer (0.5% foetal bovine serum in PBS), stained with phycoerythrin-conjugated antibodies against TRAIL receptors DR4, DR5, DcR1 and DcR2 (anti-hTRAIL R1, anti-hTRAIL R2, anti-hTRAIL R3 and anti-hTRAIL R4; R&D Systems, Minneapolis, MN, USA) and analyzed by flow cytometry in triplicate (FASCCanto II, BD Biosciences, San Jose, CA, USA). Unstained cells and cells incubated with isotype controls served as the background fluorescence controls.

Sample preparation for two-dimensional electrophoresis. HBL-2 and HBL-2/R cells ($6x10^7$) were harvested, washed twice with PBS and cell pellets were frozen and stored at -80˚C. Samples were thawed and homogenized in lysis buffer [7 M urea, 2 M thiourea, 4% CHAPS, 60 mM dithiothreitol (DTT) and 1% ampholytes (Bio-Lyte 3-10 Buffer, Bio-Rad, Hercules, CA, USA)] and protease inhibitor cocktail (Roche Diagnostics GmbH, Mannheim, Germany) for 20 min at room temperature with occasional vortexing. Samples were sedimented at 18,000 x g for 20 min at room temperature, supernatants were collected and protein concentration was determined by the Bradford assay (Bio-Rad). Protein concentrations in all samples were equalized to 3.3 mg/ml by dilution with lysis buffer.

Two-dimensional electrophoresis. IPG strips (pH 4.0-7.0, 24 cm; ReadyStrip, Bio-Rad) were rehydrated overnight in 450 μl of sample, representing 1.5 mg of protein. Isoelectric focusing was performed for 70 kVh, with maximum voltage not exceeding 5 kV, current limited to 50 μA per strip and temperature set to 20˚C (Protean IEF Cell, Bio-Rad). Six replicates were run for each cell type. Focused strips were briefly rinsed in deionized water, equilibrated and reduced in equilibration buffer supplemented with DTT (6 M urea, 50 mM Tris pH 8.8, 30% glycerol, 2% SDS and 450 mg DTT per 50 ml) for 15 min and then alkylated in equilibration buffer with iodacetamide (1.125 mg iodacetamide per 50 ml of the buffer). Equilibrated strips were then secured on 10% SDS-PAGE and secured in place by molten agarose. SDS-PAGE electrophoresis was performed in

a Tris-glycine-SDS system using a 12-gel Protean Dodeca Cell apparatus (Bio-Rad) with buffer circulation and external cooling (20˚C). Gels were run at a constant voltage of 45 V per gel for 30 min and then at a constant voltage of 200 V for 6 h. Gels were washed 3 times for 15 min in deionized water to remove redundant SDS. Gels were then stained with colloidal Coomassie Brilliant Blue (SimplyBlue™ Safestain, Invitrogen, Carlsbad, CA, USA) overnight and briefly de-stained in deionized water.

Gel image analysis and extraction of peptides. Stained gels were scanned with GS 800 calibrated densitometer (Bio-Rad) and image analysis was performed with Progenesis™ software (Nonlinear Dynamics, Ltd., Newcastle upon Tyne, UK) in semi-manual mode with 6 gel replicates for each cell type. Normalization of gel images was based on total spot density, and integrated spot density values (spot volumes) were then calculated after background subtraction. Average spot volume values (averages from the all 6 gels in the group) for each spot were compared between the groups. Protein spots were considered differentially expressed if their average normalized spot volume difference was >1.5-fold. As determined by the Student's t-test, a p-value <0.05 was considered to indicate a statistically significant difference.

Protein digestion and peptide extraction. Spots containing differentially expressed proteins were excised from the gels, cut into small pieces and washed 3 times with 25 mM ammonium bicarbonate in 50% acetonitrile (ACN). The gels were then dried in a SpeedVac Concentrator (Eppendorf, Hamburg, Germany). Sequencing grade modified trypsin (Promega, Madison, WI, USA) (6 ng/μl of trypsin in 25 mM ammonium bicarbonate in 5% ACN) was added. Following overnight incubation at 37˚C, the resulting peptides were extracted with 50% ACN.

Matrix-assisted laser desorption/ionization-time of flight mass spectrometry (MALDI-TOF MS) and identification of selected proteins. Peptide samples were spotted on a polished steel target plate (Bruker Daltonics, Bremen, Germany) and allowed to dry at room temperature. Matrix solution (3 mg α-cyano-4-hydroxycinnamic acid in 1 ml of 50% ACN containing 0.1% trifluoroacetic acid) was then added. MS was performed on an Autoflex II MALDI-TOF/TOF mass spectrometer (Bruker Daltonics) using a solid nitrogen laser (337 nm) and FlexControl software (Bruker Daltonics) in reflectron mode with positive ion mass spectra detection. The mass spectrometer was externally calibrated with Peptide Calibration Standard II (Bruker Daltonics). Spectra were acquired in the mass range 800-4,000 Da. The peak lists were generated using FlexAnalysis and searched against Swiss-Prot (2011 version, 524420 sequences) using Mascot software. The peptide mass tolerance was set to 50 ppm, taxonomy *Homo sapiens*, missed cleavage was set to 2, fixed modification for cysteine carbamidomethylation, and variable modifications for methionine oxidation and protein N-terminal acetylation.

Western blot analysis. Cells were lysed in NHT buffer (140 mM NaCl, 10 mM HEPES, 1.5% Triton X-100, pH 7.4). Protein concentration in the collected supernatants was determined by the Bradford assay (Bio-Rad). Lysate samples (25-70 μg) were combined with SDS loading buffer containing 2-mercaptoethanol and boiled for 5 min. Triplicate samples were separated on 12% SDS-PAGE minigels in Tris-glycine buffer (Bio-Rad). Electrophoresis was performed at a constant voltage for 30 min at 45 V per gel, and then at 90 V per gel until the dye front reached the gel bottom. Proteins were transferred onto 0.45 μm PVDF membranes (Milipore, Billerica, MA, USA) in a semi-dry blotter (Hoefer, San Francisco, CA, USA) at 0.8 mA/cm^2 of membrane. Membranes were incubated with blocking buffer containing PBS (Invitrogen), 0.1% Tween-20 and 5% non-fat dried milk for 1 h. As primary antibodies anti-adenine phosphoribosyltransferase (APRT; 1:1,000, rabbit polyclonal antibody), anti-purine nucleoside phosphorylase (PNP; 1:1,000, mouse monoclonal antibody) and anti-GAPDH (1:10,000, rabbit polyclonal antibody) were used. After thoroughly washing in blocking buffer, a secondary horseradish peroxidase-conjugated anti-mouse or anti-rabbit antibody was added (1:10,000). GAPDH was used as the loading control. The signal was detected using Western Blotting Luminol Reagent (Santa Cruz Biotechnology, Inc., Santa Cruz, CA, USA) and membranes were exposed to X-ray films (Kodak, Rochester, NY, USA). All used antibodies were from Santa Cruz Biotechnology.

Results

Molecular changes associated with the generation of drug-resistant cells can confer potential selective disadvantage. Such a 'weakness' may be used as druggable target for effective elimination of drug-resistant lymphoma cells. Our aim was to elucidate the molecular changes associated with the development of TRAIL resistance in (originally TRAIL-sensitive) MCL cells in order to identify such a cellular 'weakness' of TRAIL-resistant MCL cells. To identify the specific protein expression changes in the TRAIL-resistant cells, we derived a TRAIL-resistant HBL-2 subclone (HBL-2/R) from the originally TRAIL-sensitive HBL-2 cell line, and performed differential analysis of the surface expression of TRAIL receptors and comparative proteomic analysis of the HBL-2/R and HBL-2 cells.

TRAIL-resistant cell line. The TRAIL-resistant HBL-2 subclone (HBL-2/R) was derived from the originally TRAIL-sensitive HBL-2 cell line by selective pressure of increasing TRAIL concentration in medium over 5 weeks. While the IC_{50} for TRAIL in the originally sensitive HBL-2 cells was 1 ng/ml at 48 h (data not shown), the resulting HBL-2/R subclone proliferated in up to 1,000 ng/ml TRAIL concentration in medium and was therefore >1,000-fold more resistant to TRAIL than the HBL-2 cells (Fig. 1).

TRAIL receptors - flow cytometric analysis of cell surface expression. The attenuated expression of TRAIL death receptors DR4 and DR5 has been previously described as a cause of TRAIL resistance. We therefore determined the relative expression of TRAIL receptors in HBL-2 and HBL-2/R cells by flow cytometry (Fig. 2). The expression of DR4, DR5, DcR1 and DcR2 in the HBL-2/R cells was markedly decreased compared to the HBL-2 cells. The marked downregulation of death receptors DR4 and DR5 explains the resistance of the HBL-2/R cells to TRAIL, while the downregulation of decoy receptors DcR1 and DcR2 may indicate further, more complex phenotypic changes in the HBL-2/R cells.

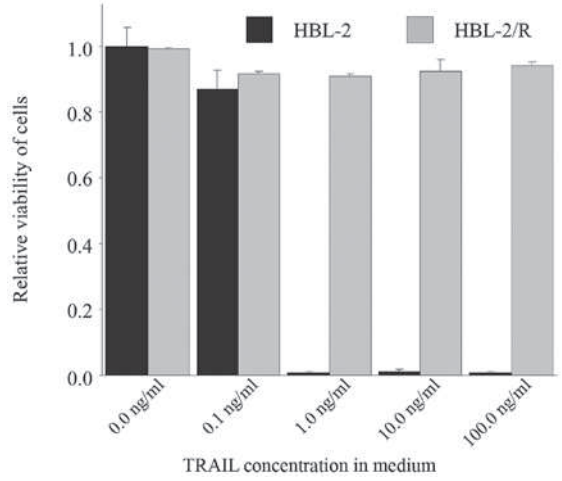

Figure 1. Relative cytotoxicity of TRAIL. Viability of TRAIL-sensitive HBL-2 cells and TRAIL-resistant HBL-2/R cells after 78 h in medium with recombinant TRAIL was determined by WTS-based colorimetric assay. Absorbance value of HBL-2 cells grown in medium without TRAIL was set to 1.

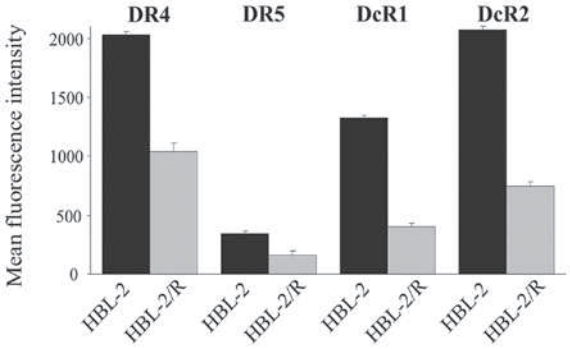

Figure 2. Cell surface expression of TRAIL receptors. HBL-2 and HBL-2/R cells were labeled with phycoerythrin-conjugated antibodies against the TRAIL cell surface receptors, DR4, DR5, DcR1 and DcR2, and the expression of the receptors was analyzed by flow cytometry. Cells without staining and isotype controls served as the blank controls.

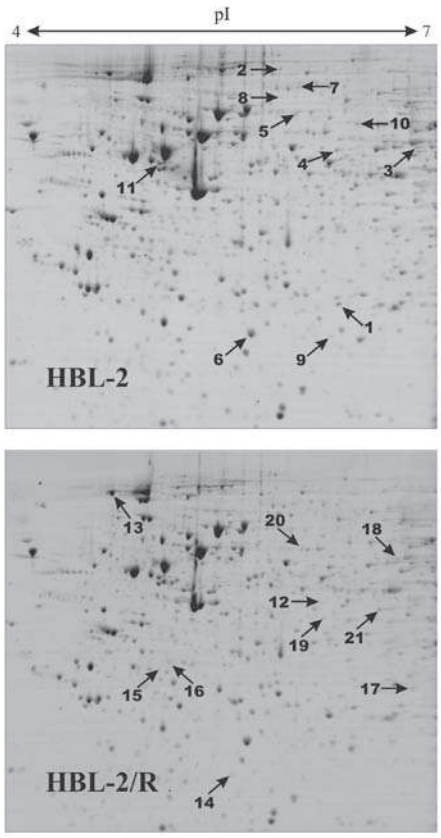

Figure 3. Two-dimensional electrophoresis of HBL-2 and HBL-2/R cells was performed on 24-cm gel strips, pH 4.0-7.0, 10% SDS-PAGE. Proteins were stained with Coomassie Brilliant Blue. Differentially expressed proteins are indicated by numbered arrows (spots 1-11 indicate downregulated proteins in HBL-2/R cells, and spots 12-21 indicate upregulated proteins in HBL-2/R cells).

Proteomic analysis. In order to identify specific changes in protein expression associated with TRAIL resistance in HBL-2/R cells, we performed comparative proteomic analysis of cellular homogenates of HBL-2/R and TRAIL-sensitive HBL-2 cells. Using two-dimensional electrophoresis of total cell lysates, we reproducibly detected 820 protein spots on Coomassie Brilliant Blue-stained gels. We found 21 protein spots to be significantly quantitatively changed (upregulated or downregulated, change >1.5-fold; $p<0.05$) in HBL-2/R cells (Fig. 3). Using MALDI-TOF/TOF mass spectrometry we identified all 21 proteins differentially expressed in HBL-2/R cells (Table I).

Functional annotations of the identified differentially expressed proteins were analyzed using the Kyoto Encyclopedia of Genes and Genomes (KEGG) database. Among the 21 identified proteins we found molecules involved in diverse functions, including cytoskeleton regulation, ribosome synthesis and maturation, RNA metabolism, chromosome translocation, DNA repair and replication, as well as protein folding. However, one pathway was markedly enriched in our set (hsa00230 - purine metabolism) represented by 3 differentially expressed proteins. These 3 molecules are key enzymes of the purine nucleotide metabolism (Fig. 5) and all 3 are downregulated in TRAIL-resistant HBL-2/R cells [PNP (downregulated 1.6-fold in HBL-2/R cells), APRT (downregulated 2.2-fold in HBL-2/R cells) and inosine-5'-monophosphate dehydrogenase 2 (IMPDH2, downregulated 1.6-fold in HBL-2/R cells)].

Verification of proteomic analysis. To confirm the results of proteomic analysis by an independent method we verified the decreased expression of the 2 proteins involved in purine metabolism, namely PNP and APRT, by western blot analysis in HBL-2 and HBL-2/R cell lysates (Fig. 4).

Discussion

The downregulation of the 3 key enzymes of purine metabolism can have a profound effect on nucleotide homeostasis in TRAIL-resistant lymphoma cells. Purine nucleotides, the building blocks for synthesis of DNA, RNA and enzyme co-factors, are recruited either from *de novo* purine synthesis from low molecular weight precursors or by recycling of free nucleobases in the so-called salvage pathway. Both pathways lead to the production of nucleoside-5'-phosphates (Fig. 5). Both pathways can supply cellular demand independently; however, their importance in different tissues is variable. In leukemic and lymphoma cells the salvage pathway is considered the major source of purine nucleotides (30,31).

Table I. List of proteins differentially expressed in HBL-2/R cells (difference at least 1.5-fold and statistical significance p<0.05).

Spot no.	Swiss-Prot no.[a]	Protein name	Fold change	Mascot score[b]	Sequence cov. (%)[c]	Mr
Proteins upregulated in HBL-2/R cells						
1	P04792	Heat shock protein β-1	3.9	84	51	22826
2	P42704	Leucine-rich PPR motif-containing protein, mitochondrial	2.6	100	23	159003
3	O75351	Vacuolar protein sorting-associated protein 4B	2.6	171	32	49443
4	P23381	Tryptophanyl-tRNA synthetase, cytoplasmic	2.4	240	54	53474
5	P20591	Interferon-induced GTP-binding protein Mx1	2.2	176	42	75872
6	P09211	Glutathione S-transferase P	1.9	110	56	23569
7	P06396	Gelsolin	1.9	115	22	86043
8	P13010	X-ray repair cross-complementing protein 5	1.7	262	46	83222
9	Q9HAV7	GrpE protein homolog 1, mitochondrial	1.6	99	44	24492
10	O43776	Asparaginyl-tRNA synthetase, cytoplasmic	1.5	250	41	63758
11	Q15084	Protein disulfide-isomerase A6	1.5	76	29	48490
Proteins downregulated in HBL-2/R cells						
12	P08559	Pyruvate dehydrogenase E1 component subunit α	3.2	111	32	43952
13	P19338	Nucleolin	2.4	146	29	76625
14	P07741	Adenine phosphoribosyltransferase	2.2	227	79	19766
15	O75792	Ribonuclease H2 subunit A	1.7	348	72	33716
16	Q07955	Serine/arginine-rich splicing factor 1	1.7	82	35	27842
17	P00491	Purine nucleoside phosphorylase	1.6	182	68	32325
18	P12268	Inosine-5'-monophosphate dehydrogenase 2	1.6	230	44	56226
19	P40121	Macrophage-capping protein	1.6	102	41	38760
20	P13674	Prolyl 4-hydroxylase subunit α-1	1.5	234	48	61296
21	Q15019	Septin-2	1.5	62	26	41689

[a]Swiss-Prot no. is the code under which the identified protein is deposited in the Swiss-Prot database. [b]Mascot score helps to estimate the correctness of the individual hit. It is expressed as -10 x log(P) where P is the probability that the observed match is a random event. [c]Sequence coverage is the number of amino acids spanned by the assigned peptides divided by the sequence length.

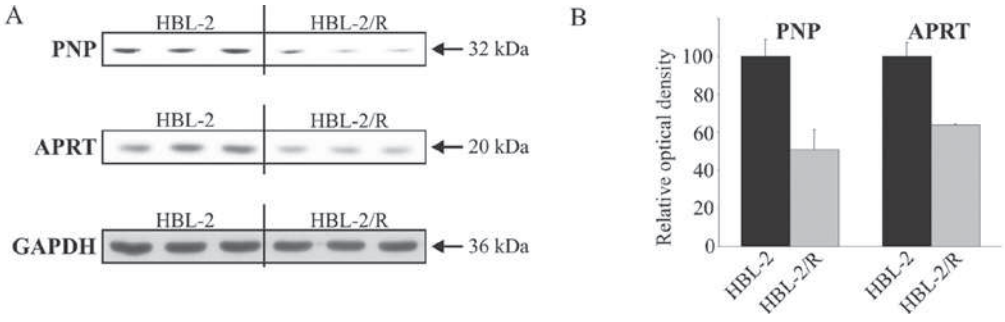

Figure 4. Relative expression of purine nucleoside phosphorylase (PNP) and adenine phosphoribosyltransferase (APRT) in HBL-2 and HBL-2/R cell lysates determined by western blot analysis. (A) Triplicate cell lysates were separated on 12% SDS-PAGE minigels. Proteins were then transferred onto PVDF membranes, blocked and probed with either anti-APRT, or anti-PNP antibody. Anti-GAPDH antibody was used as the loading control. The bands were visualized by HRP-conjugated secondary antibodies. (B) The values of integrated optical densities of PNP and APRT in HBL-2 cells were set to 100.

The *de novo* synthesis of purine nucleotides requires 5-phosphoribosyl-1-pyrophosphate (PRPP), ATP, glutamine, glycine, CO_2, aspartate and formate to create the first fully formed nucleotide, inosine-5'-monophosphate (IMP). IMP represents a branch point for purine biosynthesis, since it can be converted either to guanosine-5'-monophosphate (GMP) by IMPDH2 (downregulated in HBL-2/R cells) or to adenosine-5'-monophosphate (Fig. 5).

The catabolism of purine nucleotides leads to the liberation of free purine bases by PNP (downregulated in HBL-2/R cells). In the salvage pathway the free bases are reconverted back to nucleoside-5'-monophosphates in a reaction with activated sugar (PRPP) catalyzed by APRT (downregulated in HBL-2/R cells) or hypoxanthine-guanine phosphoribosyltransferase (32) (Fig. 5). Ribonucleotides are converted by ribonucleotide reductase into the corresponding deoxyribonucleotides.

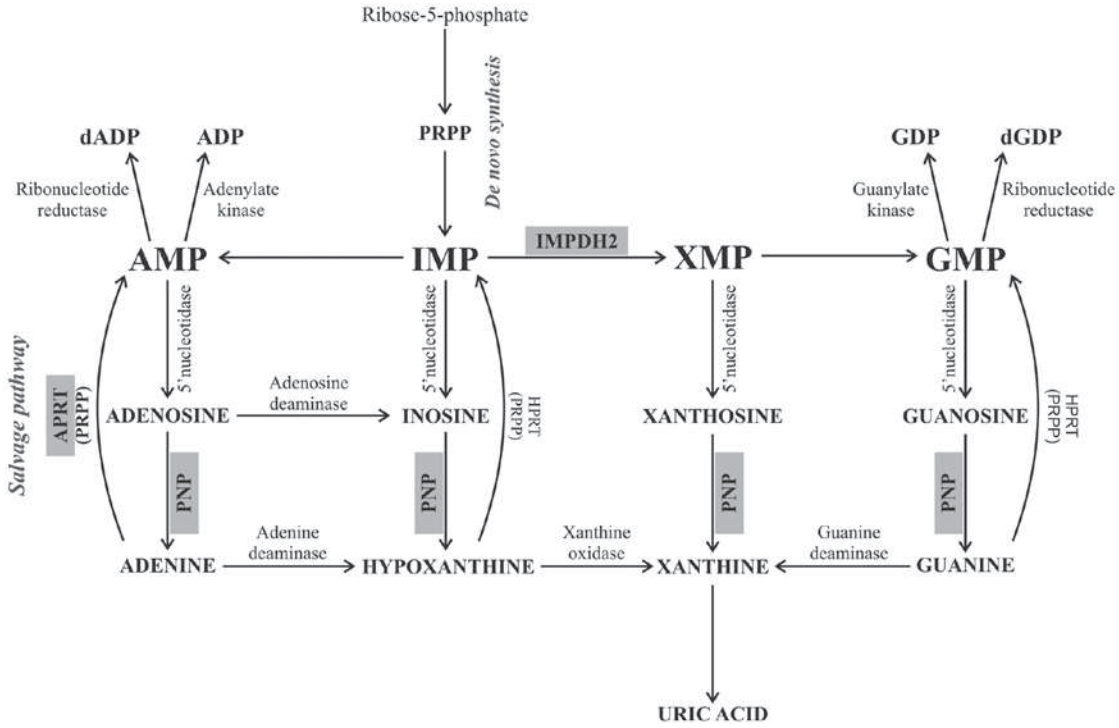

Figure 5. Scheme of the purine metabolism pathways, showing the position of IMPDH2, APRT and PNP in purine nucleotide biosynthesis, adopted from a previous study (35). The *de novo* synthesis of purine nucleotides begins with the phosphorylation of ribose-5-phosphate to form PRPP. In a number of reactions, PRPP creates the first fully formed nucleotide, IMP. IMP is converted by IMPDH2 to GMP. PNP catalyzes the reversible cleavage of purine nucleosides, releasing purine nucleobases (adenine, hypoxanthine, xanthine and guanine). In the salvage pathway the free nucleobases can be reconverted back to nucleoside-5'-monophosphates in a reaction with activated sugar (PRPP) catalyzed by APRT. IMPDH2, inosine-5'-monophosphate dehydrogenase 2; APRT, adenine phosphoribosyltransferase; PNP, purine nucleoside phosphorylase; PRPP, 5-phosphoribosyl-1-pyrophosphate; IMP, inosine-5'-monophosphate; GMP, guanosine-5'-monophosphate; dADP, deoxyadenosine diphosphate; ADP, adenosine diphosphate; GDP, guanosine diphosphate; dGDP, deoxyguanosine diphosphate; AMP, adenosine monophosphate; XMP, xanthosine monophosphate.

The delicate balance of enzyme activities and concentrations of products and intermediates are critical for purine (nucleotide) homeostasis. The inhibition of PNP results in the accumulation of its substrate, 2'-deoxyguanosine which is further phosphorylated to deoxyguanosine triphosphate (dGTP). A high intracellular concentration of dGTP inhibits cell proliferation and induces apoptosis (33-35). If APRT is inhibited, accumulated adenine is oxidized to insoluble 2,8-dihydroxyadenine. Accumulation of this precipitate results in cell death (32). Similarly, the inhibition of IMPDH2 leads to depletion of guanosine nucleotides, which blocks DNA synthesis and cell division (36,37).

Disruption of the purine nucleotide metabolism generally results in an accumulation and/or a lack of ribonucleotides or deoxyribonucleotides or metabolic intermediates with potentially cytotoxic consequences. The observed decreased expression of the 3 purine metabolism enzymes affects both *de novo* synthesis and the salvage pathway of purine metabolism and may also affect purine nucleotide homeostasis in TRAIL-resistant HBL-2/R cells. Such an imbalance may represent a selective disadvantage for the affected cells. Such a 'weakness' may not be apparent under normal circumstances but may become critical under stress or unfavorable conditions. As the proliferation rates of HBL-2/R and HBL-2 cells are comparable, the proposed imbalance in purine nucleotide metabolism in TRAIL-resistant cells is possibly mild and/or well compensated *in vitro*. However, this 'weakness' may become apparent due to lack of building blocks for DNA and RNA synthesis in the environment or upon further disruption of purine metabolism. Since both pathways of purine metabolism are compromised in TRAIL-resistant MCL cells, these cells should be vulnerable to further inactivation of purine nucleotide metabolism enzymes. Therefore, drugs that target (already disbalanced) purine metabolism should be highly cytotoxic to TRAIL-resistant cells (compared to non-malignant cells) and may therefore be selectively effective in the elimination of TRAIL-resistant MCL cells in experimental therapy. There are several approved inhibitors of purine metabolism, such as methotrexate (inhibits purine *de novo* synthesis via dihydrofolate reductase) (38), ribavirin and mycophenolic acid (inhibitors of IMPDH2) (39,40) or forodesine (a novel inhibitor of PNP) (41,42), available for clinical use.

The adaptation of cancer cells to cytostatic and cytotoxic drugs is associated to a certain degree with extensive changes in the cell phenotype. Some of the molecular changes, although seemingly unrelated to the mechanism of resistance, can provide a selective disadvantage to the cells and such a 'weakness' may be used as a potential therapeutic target. By the presented proteomic analysis of the changes associated with resistance to TRAIL in MCL HBL-2 cells, we demonstrated the downregulation of all types of TRAIL receptors and identified the altered expression of several proteins including 3 enzymes of the purine metabolism pathway. This downregulated pathway potentially represents a 'weakness' of the TRAIL-resistant MCL cells and has potential as a therapeutic target for the selective elimination of such cells in the future.

Acknowledgements

This study was supported by the Grant Agency of Charles University (GAUK 251180 111210 and 253284 700712), by the Grant Agency of the Czech Republic (305/09/1390), by the Ministry of Education, Youth and Sports (PRVOUK P24/LF1/3 and SVV 2012-264507), UNCE 204021 and the Ministry of Health of the Czech Republic (IGA MZ NT12248-5, IGA-MZ NT13201-4).

References

1. Sant M, Allemani C, Tereanu C, *et al*: Incidence of hematologic malignancies in Europe by morphologic subtype: results of the HAEMACARE project. Blood 116: 3724-3734, 2010.
2. Perez-Galan P, Dreyling M and Wiestner A: Mantle cell lymphoma: biology, pathogenesis, and the molecular basis of treatment in the genomic era. Blood 117: 26-38, 2011.
3. Tsujimoto Y, Yunis J, Onorato-Showe L, Erikson J, Nowell PC and Croce CM: Molecular cloning of the chromosomal breakpoint of B-cell lymphomas and leukemias with the t(11;14) chromosome translocation. Science 224: 1403-1406, 1984.
4. Williams ME, Swerdlow SH, Rosenberg CL and Arnold A: Characterization of chromosome 11 translocation breakpoints at the bcl-1 and PRAD1 loci in centrocytic lymphoma. Cancer Res 52: 5541S-5544S, 1992.
5. Humala K and Younes A: Current and emerging new treatment strategies for mantle cell lymphoma. Leuk Lymphoma: Feb 19, 2013 (Epub ahead of print).
6. Wiley SR, Schooley K, Smolak PJ, *et al*: Identification and characterization of a new member of the TNF family that induces apoptosis. Immunity 3: 673-682, 1995.
7. Pitti RM, Marsters SA, Ruppert S, Donahue CJ, Moore A and Ashkenazi A: Induction of apoptosis by Apo-2 ligand, a new member of the tumor necrosis factor cytokine family. J Biol Chem 271: 12687-12690, 1996.
8. Ashkenazi A and Dixit VM: Death receptors: signaling and modulation. Science 281: 1305-1308, 1998.
9. Sheridan JP, Marsters SA, Pitti RM, *et al*: Control of TRAIL-induced apoptosis by a family of signaling and decoy receptors. Science 277: 818-821, 1997.
10. Ashkenazi A: Targeting death and decoy receptors of the tumour-necrosis factor superfamily. Nat Rev Cancer 2: 420-430, 2002.
11. Castro Alves C, Terziyska N, Grunert M, *et al*: Leukemia-initiating cells of patient-derived acute lymphoblastic leukemia xenografts are sensitive toward TRAIL. Blood 119: 4224-4227, 2012.
12. Peter ME and Krammer PH: The CD95(APO-1/Fas) DISC and beyond. Cell Death Differ 10: 26-35, 2003.
13. Spierings DC: Tissue distribution of the death ligand TRAIL and its receptors. J Histochem Cytochem 52: 821-831, 2004.
14. Petrak J, Toman O, Simonova T, *et al*: Identification of molecular targets for selective elimination of TRAIL-resistant leukemia cells. From spots to in vitro assays using TOP15 charts. Proteomics 9: 5006-5015, 2009.
15. Molinsky J, Klanova M, Koc M, *et al*: Roscovitine sensitizes leukemia and lymphoma cells to tumor necrosis factor-related apoptosis-inducing ligand-induced apoptosis. Leuk Lymphoma 54: 372-380, 2013.
16. Klener P, Leahomschi S, Molinsky J, *et al*: TRAIL-induced apoptosis of HL60 leukemia cells: two distinct phenotypes of acquired TRAIL resistance that are accompanied with resistance to TNFalpha but not to idarubicin and cytarabine. Blood Cells Mol Dis 42: 77-84, 2009.
17. Leahomschi S, Molinsky J, Klanova M, *et al*: Multi-level disruption of the extrinsic apoptotic pathway mediates resistance of leukemia cells to TNF-related apoptosis-inducing ligand (TRAIL). Neoplasma 60: 223-231, 2013.
18. Wen J, Ramadevi N, Nguyen D, Perkins C, Worthington E and Bhalla K: Antileukemic drugs increase death receptor 5 levels and enhance Apo-2L-induced apoptosis of human acute leukemia cells. Blood 96: 3900-3906, 2000.
19. Plasilova M, Zivny J, Jelinek J, *et al*: TRAIL (Apo2L) suppresses growth of primary human leukemia and myelodysplasia progenitors. Leukemia 16: 67-73, 2002.
20. Ashkenazi A, Pai RC, Fong S, *et al*: Safety and antitumor activity of recombinant soluble Apo2 ligand. J Clin Invest 104: 155-162, 1999.
21. Di Pietro R and Zauli G: Emerging non-apoptotic functions of tumor necrosis factor-related apoptosis-inducing ligand (TRAIL)/Apo2L. J Cell Physiol 201: 331-340, 2004.
22. Kelley SK, Harris LA, Xie D, *et al*: Preclinical studies to predict the disposition of Apo2L/tumor necrosis factor-related apoptosis-inducing ligand in humans: characterization of in vivo efficacy, pharmacokinetics, and safety. J Pharmacol Exp Ther 299: 31-38, 2001.
23. Lawrence D, Shahrokh Z, Marsters S, *et al*: Differential hepatocyte toxicity of recombinant Apo2L/TRAIL versions. Nat Med 7: 383-385, 2001.
24. Roth W, Isenmann S, Naumann U, *et al*: Locoregional Apo2L/TRAIL eradicates intracranial human malignant glioma xenografts in athymic mice in the absence of neurotoxicity. Biochem Biophys Res Commun 265: 479-483, 1999.
25. Walczak H, Miller RE, Ariail K, *et al*: Tumoricidal activity of tumor necrosis factor-related apoptosis-inducing ligand in vivo. Nat Med 5: 157-163, 1999.
26. Hylander BL, Pitoniak R, Penetrante RB, *et al*: The anti-tumor effect of Apo2L/TRAIL on patient pancreatic adenocarcinomas grown as xenografts in SCID mice. J Transl Med 3: 22, 2005.
27. Dimberg LY, Anderson CK, Camidge R, Behbakht K, Thorburn A and Ford HL: On the TRAIL to successful cancer therapy? Predicting and counteracting resistance against TRAIL-based therapeutics. Oncogene: 14 May, 2012 (Epub ahead of print). doi: 10.1038/onc.2012.164, 2012.
28. Zhang L and Fang B: Mechanisms of resistance to TRAIL-induced apoptosis in cancer. Cancer Gene Ther 12: 228-237, 2005.
29. Maksimovic-Ivanic D, Stosic-Grujicic S, Nicoletti F and Mijatovic S: Resistance to TRAIL and how to surmount it. Immunol Res 52: 157-168, 2012.
30. Scavennec J, Maraninchi D, Gastaut JA, Carcassonne Y and Cailla HL: Purine and pyrimidine ribonucleoside monophosphate patterns of peripheral blood and bone marrow cells in human acute leukemias. Cancer Res 42: 1326-1330, 1982.
31. Natsumeda Y, Prajda N, Donohue JP, Glover JL and Weber G: Enzymic capacities of purine de novo and salvage pathways for nucleotide synthesis in normal and neoplastic tissues. Cancer Res 44: 2475-2479, 1984.
32. Bollee G, Harambat J, Bensman A, Knebelmann B, Daudon M and Ceballos-Picot I: Adenine phosphoribosyltransferase deficiency. Clin J Am Soc Nephrol 7: 1521-1527, 2012.
33. Bantia S, Miller PJ, Parker CD, *et al*: Purine nucleoside phosphorylase inhibitor BCX-1777 (Immucillin-H) - a novel potent and orally active immunosuppressive agent. Int Immunopharmacol 1: 1199-1210, 2001.
34. Bantia S, Montgomery JA, Johnson HG and Walsh GM: In vivo and in vitro pharmacologic activity of the purine nucleoside phosphorylase inhibitor BCX-34: the role of GTP and dGTP. Immunopharmacology 35: 53-63, 1996.
35. Galmarini CM, Popowycz F and Joseph B: Cytotoxic nucleoside analogues: different strategies to improve their clinical efficacy. Curr Med Chem 15: 1072-1082, 2008.
36. Allison AC and Eugui EM: Mycophenolate mofetil and its mechanisms of action. Immunopharmacology 47: 85-118, 2000.
37. Hedstrom L: IMP dehydrogenase: structure, mechanism, and inhibition. Chem Rev 109: 2903-2928, 2009.
38. Fairbanks LD, Ruckemann K, Qiu Y, *et al*: Methotrexate inhibits the first committed step of purine biosynthesis in mitogen-stimulated human T-lymphocytes: a metabolic basis for efficacy in rheumatoid arthritis? Biochem J 342: 143-152, 1999.
39. Allison AC and Eugui EM: The design and development of an immunosuppressive drug, mycophenolate mofetil. Springer Semin Immunopathol 14: 353-380, 1993.
40. Zhou S, Liu R, Baroudy BM, Malcolm BA and Reyes GR: The effect of ribavirin and IMPDH inhibitors on hepatitis C virus subgenomic replicon RNA. Virology 310: 333-342, 2003.
41. Gandhi V, Kilpatrick JM, Plunkett W, *et al*: A proof-of-principle pharmacokinetic, pharmacodynamic, and clinical study with purine nucleoside phosphorylase inhibitor immucillin-H (BCX-1777, forodesine). Blood 106: 4253-4260, 2005.
42. Miles RW, Tyler PC, Furneaux RH, Bagdassarian CK and Schramm VL: One-third-the-sites transition-state inhibitors for purine nucleoside phosphorylase. Biochemistry 37: 8615-8621, 1998.